MODELING OF POWER COMPONENTS FOR TRANSIENT ANALYSIS

Juan A. Martinez-Velasco
Universitat Politècnica de Catalunya, Barcelona, Spain

Juri Jatskevich
University of British Columbia, Vancouver, Canada

Shaahin Filizadeh
University of Manitoba, Winnipeg, Canada

Marjan Popov
Delft University of Technology, Delft, The Netherlands

Michel Rioual
Électricité de France R & D, Clamart, France

José L. Naredo
CINVESTAV, Guadalajara, Mexico

Keywords: Power system transients, electromagnetic transients, overhead line, insulated cable, transformer, rotating machine, synchronous machine, induction machine, modeling, frequency range, wide-band model, simulation, solution technique.

Contents

Summary

Models of power components for electromagnetic transient analysis are derived by taking into account the frequency range of the transient to be analyzed and the frequency-dependence of some parameters. Since an accurate representation for the whole frequency range of transients is very difficult and for most components is not practically possible, modeling of power components is usually made by developing models which are accurate enough for a specific range of frequencies; each range of frequencies corresponds to some particular transient phenomena. This chapter presents a summary of the guidelines proposed in the literature for representing power components when analyzing electromagnetic transients in power systems. Since the simulation of a transient phenomenon implies not only the selection of models but the selection of the system area, some rules to be considered for this purpose are also provided. The chapter discusses the models to be used in electromagnetic transient studies for some of the most common and important power components; namely, overhead lines, insulated

cables, transformers and rotating machines. The approach used for studying each component depends basically of the way in which the parameters to be specified in the transient models are to be obtained. The chapter summarizes the approaches to be used for representing each component taking into the frequency range of transients, and provides the procedures for obtaining the parameters of those components for which their values are usually derived from geometry (i.e., overhead lines and insulated cables).

1. Introduction

An accurate representation of a power component is essential for reliable transient analysis. The simulation of transient phenomena may require a representation of network components valid for a frequency range that varies from DC to several MHz. Although the ultimate objective in research is to provide wideband models, an acceptable representation of each component throughout this frequency range is very difficult, and for most components is not practically possible. In some cases, even if the wideband version is available, it may exhibit computational inefficiency or require very complex data (Martinez-Velasco, 2009).

Modeling of power components taking into account the frequency-dependence of parameters can be currently achieved through mathematical models which are accurate enough for a specific range of frequencies. Each range of frequencies usually corresponds to some particular transient phenomena. One of the most accepted classifications divides frequency ranges into four groups (IEC 60071-1, 2010; CIGRE WG 33.02, 1990): low-frequency oscillations, from 0.1 Hz to 3 kHz, slow-front surges, from 50/60 Hz to 20 kHz, fast-front surges, from 10 kHz to 3 MHz, very fast-front surges, from 100 kHz to 50 MHz. One can note that there is overlap between frequency ranges.

If a representation is already available for each frequency range, the selection of the model may suppose an iterative procedure: the model must be selected based on the frequency range of the transients to be simulated; however, the frequency ranges of the case study are not usually known before performing the simulation. This task can be alleviated by looking into widely accepted classification tables. Table 1 shows a short list of common transient phenomena.

Origin	Frequency Range
Ferroresonance	0.1 Hz - 1 kHz
Load rejection	0.1 Hz - 3 kHz
Fault clearing	50 Hz - 3 kHz
Line switching	50 Hz - 20 kHz
Transient recovery voltages	50 Hz - 100 kHz
Lightning overvoltages	10 kHz - 3 MHz
Disconnector switching in GIS	100 kHz - 50 MHz

Table 1. Origin and frequency ranges of transients in power systems

An important effort has been dedicated to clarify the main aspects to be considered when representing power components in transient simulations. Users of electromagnetic transients (EMT) tools can nowadays obtain information on this field from several sources:

a) The document written by the CIGRE WG 33-02 covers the most important power components and proposes the representation of each component taking into account the frequency range of the transient phenomena to be simulated (CIGRE WG 33.02, 1990).
b) The documents produced by the IEEE WG on Modeling and Analysis of System Transients Using Digital Programs and its Task Forces present modeling guidelines for several particular types of studies (Gole, Martinez-Velasco, & Keri, 1998).
c) The fourth part of the IEC 60071 (TR 60071-4) provides modeling guidelines for insulation coordination studies when using numerical simulation; e.g., EMTP-like tools (IEC TR 60071-4, 2004). EMTP is an acronym that stands for ElectroMagnetic Transients Program.

Table 2 provides a summary of modeling guidelines for the representation of the power components analyzed in this chapter taking into account the frequency range of transient phenomena.

Component	**Low-Frequency Transients 0.1 HZ - 3 kHz**	**Slow-Front Transients 50 Hz - 20 kHz**	**Fast-Front Transients 10 kHz - 3MHz**	**Very Fast-Front Transients 100 kHz - 50 MHz**
Overhead Lines	Multi-phase model with lumped and constant parameters, including conductor asymmetry. Frequency-dependence of parameters can be important for the ground propagation mode. Corona effect can be also important if phase conductor voltages exceed the corona inception voltage.	Multi-phase model with distributed parameters, including conductor asymmetry. Frequency-dependence of parameters is important for the ground propagation mode.	Multi-phase model with distributed parameters, including conductor asymmetry and corona effect. Frequency-dependence of parameters is important for the ground propagation mode.	Single-phase model with distributed parameters. Frequency-dependence of parameters is important for the ground propagation mode.
Insulated Cables	Multi-phase model with lumped and constant parameters, including conductor asymmetry. Frequency-dependence of parameters can be important for the ground propagation mode.	Multi-phase model with distributed parameters, including conductor asymmetry. Frequency-dependence of parameters is important for the ground propagation mode	Multi-phase model with distributed parameters. Frequency-dependence of parameters is important for the ground propagation mode.	Single-phase model with distributed parameters. Frequency-dependence of parameters is important for the ground propagation mode.

Transformers	Models must incorporate saturation effects, as well as core and winding losses. Models for single- and three-phase core can show significant differences.	Models must incorporate saturation effects, as well as core and winding losses. Models for single- and three-phase core can show significant differences.	Core losses and saturation can be neglected. Coupling between phases is mostly capacitive. The influence of the short-circuit impedance can be significant.	Core losses and saturation can be neglected. Coupling between phases is mostly capacitive. The model should incorporate the surge impedance of windings.
Rotating Machines	Detailed representation of the electrical and mechanical parts, including saturation effects and control units for synchronous machines.	The machine is represented as a source in series with its subtransient impedance. Saturation effects can be neglected. The mechanical part and control units are not included.	The representation is based on a linear circuit whose frequency response matches that of the machine seen from its terminals.	The representation may be based on a linear lossless capacitive circuit.

Table 2. Modeling of power components for transient simulations

The simulation of a transient phenomenon implies not only the selection of models but the selection of the system area that must be represented. Some rules to be considered in the simulation of electromagnetic transients when selecting models and the system area can be summarized as follows (Martinez-Velasco, 2009):

1) Select the system zone taking into account the frequency range of the transients; the higher the frequencies, the smaller the zone modeled.
2) Minimize the part of the system to be represented. An increased number of components does not necessarily mean increased accuracy, since there could be a higher probability of insufficient or wrong modeling. In addition, a very detailed representation of a system will usually require longer simulation time.
3) Implement an adequate representation of losses. Since their effect on maximum voltages and oscillation frequencies is limited, they do not play a critical role in many cases. There are, however, some cases (e.g., ferro-resonance or capacitor bank switching) for which losses are critical to defining the magnitude of overvoltages.
4) Consider an idealized representation of some components if the system to be simulated is too complex. Such representation will facilitate the edition of the data file and simplify the analysis of simulation results.
5) Perform a sensitivity study if one or several parameters cannot be accurately determined. Results derived from such study will show what parameters are of concern.

This chapter is dedicated to present the models to be used in electromagnetic transient studies for the power components analyzed in Table 2. The treatment is different for each component:

- The sections dedicated to Overhead Lines and Insulated Cables discuss the representations to be considered for each frequency range, summarize the calculation of electrical parameters, and introduce the main techniques proposed for solving the mathematical equations. A short description of the routines implemented in EMT tools for calculation of parameters and creation of models is also included in each section.

- Each of the sections dedicated to Transformers and Rotating Machines is basically divided into two parts respectively dedicated to summarize the models to be used in low- and high-frequency transient studies.

2. Overhead Lines

2.1. Introduction

Simulation of electromagnetic transients can be of vital importance when analyzing the interaction of overhead lines with other power components and for overhead line design. The selection of an adequate line model is required in many transient studies; e.g., overvoltages and insulation coordination studies, power quality, protection or secondary arc studies.

Voltage stresses to be considered in overhead line design can be also classified into groups each one having a different frequency range (IEC 60071-2, 1996; IEEE Std 1313.2, 1999; Hileman, 1999): (i) power-frequency voltages in the presence of contamination; (ii) temporary (low-frequency) overvoltages produced by faults, load rejection or ferro-resonance; (iii) slow-front overvoltages produced by switching or disconnecting operations; (iv) fast-front overvoltages, generally caused by lightning flashes. For some of the required specifications, only one of these stresses is of major importance. For example, lightning will dictate the location and number of shield wires, and the design of tower grounding. The arrester rating is determined by temporary overvoltages, whilst the type of insulators will be dictated by the contamination. However, in other specifications, two or more of the overvoltages must be considered. For example, switching overvoltages, lightning, or contamination may dictate the strike distances and insulator string length. In transmission lines, contamination may determine the insulator string creepage length, which may be longer than that obtained from switching or lightning overvoltages. In general, switching surges are important only for voltages of 345 kV and above; for lower voltages, lightning dictates larger clearances and insulator lengths than switching overvoltages do. However, this may not be always true for compact designs (Hileman, 1999).

Two types of time-domain models have been developed for overhead lines: lumped- and distributed-parameter models. The appropriate selection of a model depends on the highest frequency involved in the phenomenon under study and, to less extent, on the line length.

Lumped-parameter line models represent transmission systems by lumped R, L, G and C elements whose values are calculated at a single frequency. These models, known as π-models, are adequate for steady-state calculations, although they can also be used for transient simulations in the neighborhood of the frequency at which parameters were evaluated. The most accurate models for transient calculations are those that take into account the distributed nature of the line parameters (CIGRE WG 33.02, 1990; Gole, Martinez-Velasco, & Keri, 1998; IEC TR 60071-4, 2004). Two categories can be distinguished for these models: constant parameters and frequency-dependent parameters.

The number of spans and the different hardware of a transmission line, as well as the models required to represent each part (conductors and shield wires, towers, grounding, insulation), depend on the voltage stress cause. The following rules summarize the modeling guidelines to be followed in each case (Martinez-Velasco, Ramirez, & Dávila, 2009).

1. In power-frequency and temporary overvoltage calculations, the whole transmission line length must be included in the model, but only the representation of phase conductors is needed. A multi-phase model with lumped and constant parameters, including conductor asymmetry, will generally suffice. For transients with a frequency range above 1 kHz, a frequency-dependent model could be needed to account for the ground propagation mode. Corona effect can be also important if phase conductor voltages exceed the corona inception voltage.
2. In switching overvoltage calculations, a multi-phase distributed-parameter model of the whole transmission line length, including conductor asymmetry, is in general required. As for temporary overvoltages, frequency-dependence of parameters is important for the ground propagation mode, and only phase conductors need to be represented.
3. The calculation of lightning-caused overvoltages requires a more detailed model, in which towers, footing impedances, insulators and tower clearances, in addition to phase conductors and shield wires, are represented. However, only a few spans at both sides of the point of impact must be considered in the line model. Since lightning is a fast-front transient phenomenon, a multi-phase model with distributed parameters, including conductor asymmetry and corona effect, is required for the representation of each span.

Note that the length extent of an overhead line that must be included in a model depends on the type of transient to be analyzed. As a rule of thumb, the lower the frequencies, the more length of line to be represented. For low- and mid-frequency transients, the whole line length is included in the model. For fast-front and very fast-front transients, a few line spans will usually suffice. These guidelines are illustrated in Figure 1 and summarized in Table 3, which provides modeling guidelines for overhead lines proposed in the literature (CIGRE WG 33.02, 1990; Gole, Martinez-Velasco, & Keri, 1998; IEC TR 60071-4, 2004).

The following subsections are respectively dedicated to present the line equations and the calculation of the electrical parameters to be specified in these equations, discuss the techniques proposed for the solution of these equations, and report the main features of routines implemented in most EMT tools for the calculation of line parameters (impedance and admittance) and the development of line models to be used in different transient phenomena (see Figure 1).

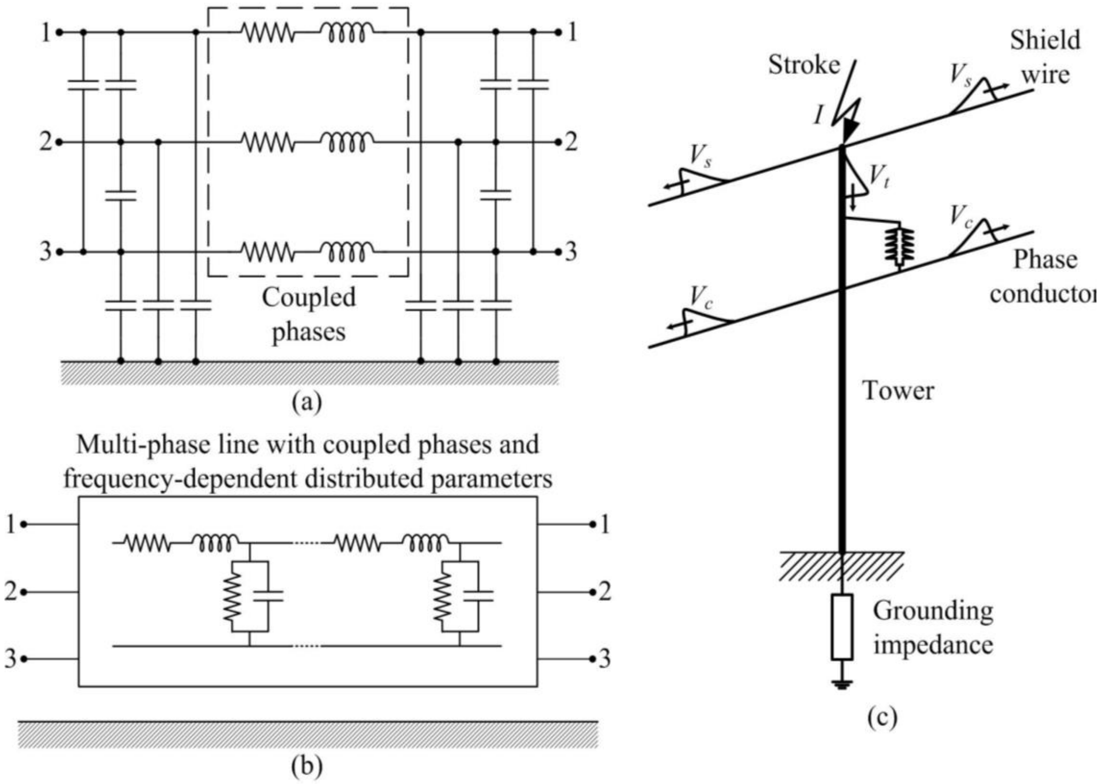

Figure 1. Line models for different ranges of frequency. (a) Steady state and low-frequency transients. (b) Switching (slow-front) transients. (c) Lightning (fast-front) transients.

TOPIC	Low-Frequency Transients	Slow-Front Transients	Fast-Front Transients	Very Fast-Front Transients
Representation of transposed lines	Lumped-parameter multi-phase pi circuit	Distributed-parameter multi-phase model	Distributed-parameter multi-phase model	Distributed-parameter single-phase model
Line asymmetry	Important	Capacitive and inductive asymmetries are important, except for statistical studies, for which they are negligible	Negligible for single-phase simulations, otherwise important	Negligible
Frequency-dependent parameters	Important	Important	Important	Important
Corona effect	Important if phase conductor voltages can exceed the corona inception voltage	Negligible	Very important	Negligible
Supports	Not important	Not important	Very important	Depends on the cause of transient

Grounding	Not important	Not important	Very important	Depends on the cause of transient
Insulators	Not included, unless flashovers are to be simulated			

Table 3. Modeling guidelines for overhead lines

2.2. Transmission Line Equations

Figure 2 depicts a differential section of a three-phase unshielded overhead line illustrating the couplings among series inductances and among shunt capacitances. The behavior of a multi-conductor overhead line is described in the frequency domain by two matrix equations:

$$-\frac{d\mathbf{V}_x(\omega)}{dx} = \mathbf{Z}(\omega)\,\mathbf{I}_x(\omega) \tag{1a}$$

$$-\frac{d\mathbf{I}_x(\omega)}{dx} = \mathbf{Y}(\omega)\,\mathbf{V}_x(\omega) \tag{1b}$$

where $\mathbf{Z}(\omega)$ and $\mathbf{Y}(\omega)$ are respectively the series impedance and the shunt admittance matrices per unit length.

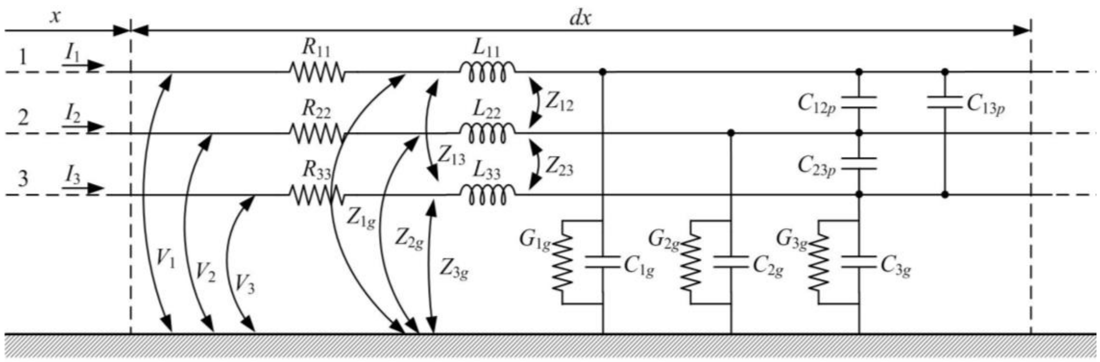

Figure 2. Differential section of a three-phase overhead line.

The series impedance matrix of an overhead line can be decomposed as follows:

$$\mathbf{Z}(\omega) = \mathbf{R}(\omega) + j\omega\mathbf{L}(\omega) \tag{2}$$

where $\mathbf{Z}$ is a complex and symmetric matrix, whose elements are frequency-dependent. For transient analysis, elements of $\mathbf{R}$ and $\mathbf{L}$ must be calculated taking into account the skin effect in conductors and in the ground. For aerial lines this is achieved by using either Carson's ground impedance (Carson, 1926) or Schelkunoff's surface impedance formulae for cylindrical conductors (Schelkunoff, 1934). For a description of the procedures see (Dommel, 1986).

The shunt admittance can be expressed as follows:

$$\mathbf{Y}(\omega) = \mathbf{G} + j\omega\mathbf{C} \tag{3}$$

where $\mathbf{Y}$ is also a complex and symmetric matrix, with frequency-dependent elements. Those of $\mathbf{G}$ may be associated with currents leaking to ground through insulator strings, which can mainly occur with polluted insulators. Their values can usually be neglected for most studies; however, under corona effect conductance values can be significant. That is, under non-corona conditions, with clean insulators and dry weather, conductances can be neglected. As for $\mathbf{C}$ elements, their frequency dependence can be neglected within the frequency range that is of concern for overhead line design (Dommel, 1986).

If parameter matrices $\mathbf{R}$, $\mathbf{L}$, $\mathbf{G}$ and $\mathbf{C}$ can be considered constant (i.e., independent of frequency), Eqs. (1a) and (1b) can be stated as follows:

$$-\frac{\partial \mathbf{v}(x,t)}{\partial x} = \mathbf{R}\mathbf{i}(x,t) + \mathbf{L}\frac{\partial \mathbf{i}(x,t)}{\partial t} \tag{4a}$$

$$-\frac{\partial \mathbf{i}(x,t)}{\partial x} = \mathbf{G}\mathbf{v}(x,t) + \mathbf{C}\frac{\partial \mathbf{v}(x,t)}{\partial t} \tag{4b}$$

where $\mathbf{v}(x,t)$ and $\mathbf{i}(x,t)$ are respectively the voltage and the current vectors. These two expressions are often referred to as the modified telegrapher's equations for multi-conductor lines.

Advanced models can consider an additional distance-dependence of the line parameters (non-uniform line), the effect of induced voltages due to distributed sources caused by nearby lightning (illuminated line), and the dependence of the line capacitance with respect to the voltage (nonlinear line, due to corona effect). Given the frequency dependence of the series parameters, the approach to the solution of the line equations, even in transient calculations, is performed in the frequency domain. This chapter presents in detail the case of the frequency-dependent uniform line (Martinez-Velasco, Ramirez, & Dávila, 2009).

2.3. Calculation of Line Parameters

2.3.1. Shunt Capacitance Matrix

On neglecting the penetration of transversal electric fields in the ground and in the conductors, the capacitance matrix can be considered as a function of the transversal geometry of the line and of the electric permittivity of the line insulators which for overhead lines is the air. Consider a configuration of n arbitrary wires in the air over a perfectly conducting ground. The assumption of the ground being a perfect conductor allows the application of the method of electrostatic images, as shown in Figure 3.

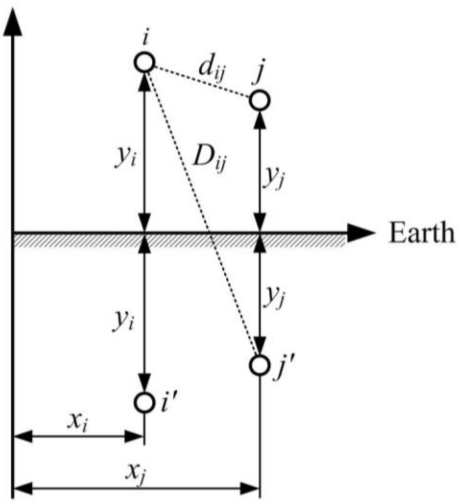

Figure 3 Application of the method of images.

The potential vector of the conductors with respect to ground due to the charges on all of them is:

$$\mathbf{v} = \mathbf{P}\,\mathbf{q} \tag{5}$$

where $\mathbf{v}$ is the vector of voltages applied to the conductors, $\mathbf{q}$ is the vector of linear densities of electric charges at each conductor and $\mathbf{P}$ is the matrix of potential coefficients of Maxwell whose elements are given by (Galloway, Shorrocks, & Wedepohl, 1964):

$$\mathbf{P} = \frac{1}{2\pi\varepsilon_0}\begin{bmatrix} \ln\dfrac{D_{11}}{r_1} & \cdots & \ln\dfrac{D_{1n}}{d_{1n}} \\ \vdots & \ddots & \vdots \\ \ln\dfrac{D_{n1}}{d_{n1}} & \cdots & \ln\dfrac{D_{nn}}{r_n} \end{bmatrix} \tag{6}$$

where ε_0 is the permittivity of the air or of free space, r_i is the radius of the i-th conductor and (see Figure 3)

$$D_{ij} = \sqrt{\left(x_i - x_j\right)^2 + \left(y_i + y_j\right)^2} \quad d_{ij} = \sqrt{\left(x_i - x_j\right)^2 + \left(y_i - y_j\right)^2} \tag{7}$$

When calculating electrical parameters of transmission lines with bundled conductors r_i must be substituted by the geometric mean radius of the bundle:

$$R_{\mathrm{eq},i} = \sqrt[n]{n\, r_i \left(r_{\mathrm{b}}\right)^{n-1}} \tag{8}$$

being n the number of conductors and r_{b} the radius of the bundle.

Finally, the capacitance matrix is calculated by inverting the matrix of potential coefficients:

$$\mathbf{C} = \mathbf{P}^{-1} \tag{9}$$

2.3.2. Series Impedance Matrix

The series or longitudinal impedance matrix is computed from the geometric and electric characteristics of the transmission line. In general, it can be decomposed into two terms:

$$\mathbf{Z} = \mathbf{Z}_{\text{ext}} + \mathbf{Z}_{\text{int}} \tag{10}$$

where $\mathbf{Z}_{\text{ext}}$ and $\mathbf{Z}_{\text{int}}$ are respectively the external and the internal series impedance matrix.

The external impedance accounts for the magnetic field exterior to the conductor and comprises the contributions of the magnetic field in the air ($\mathbf{Z}_g$) and the field penetrating the earth ($\mathbf{Z}_e$).

External series impedance matrix: The contribution of the earth return path is a very important component of the series impedance matrix. Carson reported the earliest solution of the problem of a thin wire above earth (Carson, 1926). Carson expressions for earth impedances are given as a pair of integrals that are not easy to handle. Simpler formulas to approximate Carson solutions are those obtained by using the Complex Image method (Gary, 1976), which consists in replacing the lossy ground by a perfect conductive line at a complex depth. Deri, Tevan, Semlyen, & Castanheira (1981) demonstrated that these formulas provide accurate approximations to Carson integrals and extended them to the case of multi-layer ground return.

Consider again a configuration of *n* arbitrary wires in the air over a lossy ground. Using the complex image method (see Figure 4) the external impedance matrix can be written as follows:

$$\mathbf{Z}_{\text{ext}} = j\omega \frac{\mu_0}{2\pi} \begin{bmatrix} \ln \dfrac{D'_{11}}{r_1} & \cdots & \ln \dfrac{D'_{1n}}{d_{1n}} \\ \vdots & \ddots & \vdots \\ \ln \dfrac{D'_{n1}}{d_{n1}} & \cdots & \ln \dfrac{D'_{nn}}{r_n} \end{bmatrix} \tag{11}$$

where

$$D'_{ij} = \sqrt{\left(x_i - x_j\right)^2 + \left(y_i + y_j + 2p\right)^2} \tag{12}$$

and the complete depth p is given by:

$$p = \sqrt{\frac{1}{j\omega\mu_{\mathrm{e}}(\sigma_{\mathrm{e}} + j\omega\varepsilon_{\mathrm{e}})}} \tag{13}$$

where σ_{e}, μ_{e} and ε_{e} are the ground conductivity (S/m), permeability (H/m) and permittivity (F/m), respectively.

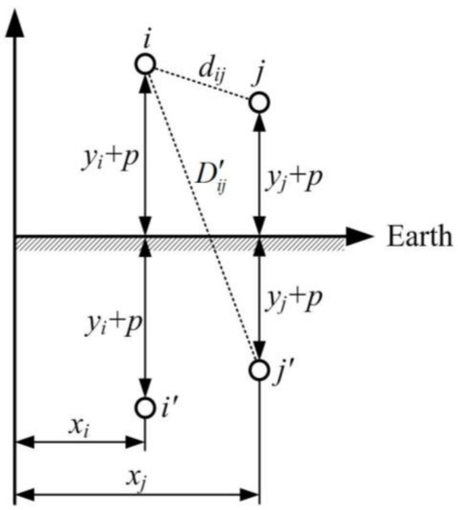

Figure 4. Geometry of the complex images.

Multiplying each element of (11) by D_{ij} / D_{ij}, the external impedance can be cast in terms of the geometrical impedance, $\mathbf{Z}_{\mathrm{g}}$, and the earth return impedance, $\mathbf{Z}_{\mathrm{e}}$:

$$\mathbf{Z}_{\mathrm{ext}} = \mathbf{Z}_g + \mathbf{Z}_{\mathrm{e}} \tag{14}$$

where

$$\mathbf{Z}_{\mathrm{g}} = j\omega\frac{\mu_0}{2\pi}\begin{bmatrix} \ln\frac{D_{11}}{r_1} & \cdots & \ln\frac{D_{1n}}{d_{1n}} \\ \vdots & \ddots & \vdots \\ \ln\frac{D_{n1}}{d_{n1}} & \cdots & \ln\frac{D_{nn}}{r_n} \end{bmatrix} \mathbf{Z}_{\mathrm{e}} = j\omega\frac{\mu_0}{2\pi}\begin{bmatrix} \ln\frac{D'_{11}}{D_{11}} & \cdots & \ln\frac{D'_{1n}}{D_{1n}} \\ \vdots & \ddots & \vdots \\ \ln\frac{D'_{n1}}{D_{n1}} & \cdots & \ln\frac{D'_{nn}}{D_{nn}} \end{bmatrix} \tag{15}$$

Internal series impedance: When the wires are not perfect conductors the total tangential electric field in the wires is not zero; that is, there is a penetration of the electric field into the conductor. This phenomenon is taken into account by adding the internal impedance. The internal impedance of a round wire is found from the total current in the wire and the electric field intensity at the surface (surface impedance):

$$Z_{\text{int}} = -\frac{Z_{\text{cw}}}{2\pi r_{\text{c}}} \frac{I_0(\gamma_{\text{c}} r_{\text{c}})}{I_1(\gamma_{\text{c}} r_{\text{c}})} \tag{16}$$

where $I_0(.)$ and $I_1(.)$ are modified Bessel functions, Z_{cw} is the wave impedance in the conductor given by:

$$Z_{\text{cw}} = \sqrt{j\omega \frac{\mu_{\text{c}}}{\sigma_{\text{c}} + j\omega\varepsilon_{\text{c}}}} \tag{17}$$

and γ_{c} is the propagation constant in the conducting material,

$$\gamma_{\text{c}} = \sqrt{j\omega\mu_{\text{c}}(\sigma_{\text{c}} + j\omega\varepsilon_{\text{c}})} \tag{18}$$

The conductivity, permittivity, permeability and the radius of the conductor are denoted by σ_{c}, ε_{c}, μ_{c}, r_{c}.

For the case of bundled conductors Z_{int} can be calculated by first evaluating (16) for one of the conductors in the bundle and then dividing this result by the number of bundled conductors. The internal impedance matrix for a multi-conductor line with *n* phases is defined as follows:

$$\mathbf{Z}_{\text{int}} = \text{diag}\left(Z_{\text{int},1}, Z_{\text{int},2}, \ldots, Z_{\text{int},n}\right) \tag{19}$$

Formulas for the internal impedance that take into account the stranding of real power conductors were provided by Galloway, Shorrocks, & Wedepohl (1964) and Gary (1976).

2.4. Solution of Line Equations

2.4.1. General Solution

The general solution of the line equations in the frequency domain can be expressed as follows:

$$\mathbf{I}_x(\omega) = e^{-\Gamma(\omega)x}\mathbf{I}_{\text{f}}(\omega) + e^{+\Gamma(\omega)x}\mathbf{I}_{\text{b}}(\omega) \tag{20a}$$
$$\mathbf{V}_x(\omega) = \mathbf{Y}_{\text{c}}^{-1}(\omega)[e^{-\Gamma(\omega)x}\mathbf{I}_{\text{f}}(\omega) - e^{+\Gamma(\omega)x}\mathbf{I}_{\text{b}}(\omega)] \tag{20b}$$

where $\mathbf{I}_{\text{f}}(\omega)$ and $\mathbf{I}_{\text{b}}(\omega)$ are the vectors of forward and backward traveling wave currents at x = 0, $\mathbf{\Gamma}(\omega)$ is the propagation constant matrix and $\mathbf{Y}_{\text{c}}(\omega)$ is the characteristic admittance matrix given by:

$$\mathbf{\Gamma}(\omega) = \sqrt{\mathbf{YZ}} \tag{21}$$

and

$$\mathbf{Y}_\mathrm{c}(\omega) = \sqrt{(\mathbf{YZ})^{-1}\mathbf{Y}} \tag{22}$$

$\mathbf{I}_\mathrm{f}(\omega)$ and $\mathbf{I}_\mathrm{b}(\omega)$ can be deduced from the boundary conditions of the line. Considering the frame shown in Figure 5, the solution at line ends can be formulated as follows:

$$\mathbf{I}_k(\omega) = \mathbf{Y}_\mathrm{c}(\omega)\mathbf{V}_k(\omega) - \mathbf{H}(\omega)\left[\mathbf{Y}_\mathrm{c}(\omega)\mathbf{V}_m(\omega) + \mathbf{I}_m(\omega)\right] \tag{23a}$$

$$\mathbf{I}_m(\omega) = \mathbf{Y}_\mathrm{c}(\omega)\mathbf{V}_m(\omega) - \mathbf{H}(\omega)\left[\mathbf{Y}_\mathrm{c}(\omega)\mathbf{V}_k(\omega) + \mathbf{I}_k(\omega)\right] \tag{23b}$$

where $\mathbf{H} = \exp(-\mathbf{\Gamma}\ell)$, being ℓ the length of the line.

Transforming Eqs. (23) into the time domain gives:

$$\mathbf{i}_k(t) = \mathbf{y}_\mathrm{c}(t) * \mathbf{v}_k(t) - \mathbf{h}(t) * \left\{\mathbf{y}_\mathrm{c}(t) * \mathbf{v}_m(t) + \mathbf{i}_m(t)\right\} \tag{24a}$$

$$\mathbf{i}_m(t) = \mathbf{y}_c(t) * \mathbf{v}_m(t) - \mathbf{h}(t) * \left\{\mathbf{y}_c(t) * \mathbf{v}_k(t) + \mathbf{i}_k(t)\right\} \tag{24b}$$

where symbol $*$ indicates convolution and $\mathbf{x}(t) = \mathrm{F}^{-1}\left\{\mathbf{X}(\omega)\right\}$ is the inverse Fourier transform.

These equations suggest that an overhead line can be represented at each end by a multi-terminal admittance paralleled by a multi-terminal current source, as shown in Figure 6.

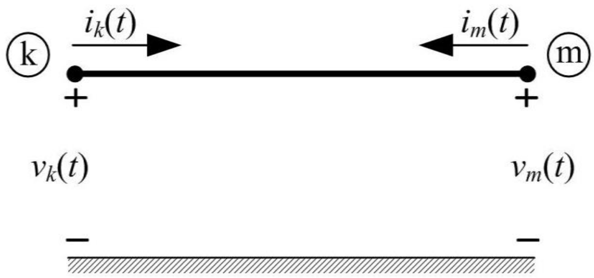

Figure 5. Line model - Reference frame.

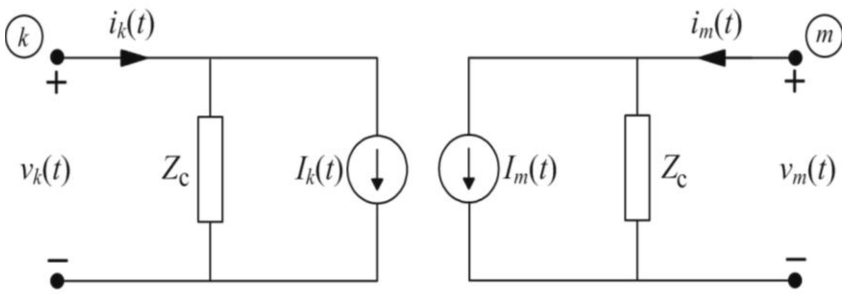

Figure 6. Equivalent circuit for time-domain simulations.

The implementation of this equivalent circuit requires the synthesis of an electrical network to represent the multi-terminal admittance. In addition, the current source values have to be updated at every time step during the time-domain calculation. Both tasks are not straightforward, and many approaches have been developed to cope with this problem.

The techniques developed to solve the equations of a multi-conductor frequency-dependent overhead line can be classified into two main categories: modal-domain techniques and phase-domain techniques. An overview of the main approaches is presented below (Martinez-Velasco, Ramirez, & Dávila, 2009).

2.4.2. Modal-domain Solution Techniques

Overhead line equations can be solved by introducing a new reference frame:

$$\mathbf{V}_{\mathrm{ph}} = \mathbf{T}_{\mathrm{v}}\ \mathbf{V}_{\mathrm{m}} \tag{25a}$$

$$\mathbf{I}_{\mathrm{ph}} = \mathbf{T}_{\mathrm{i}}\ \mathbf{I}_{\mathrm{m}} \tag{25b}$$

where the subscripts ph and m refer to the original phase quantities and the new modal quantities. Matrices $\mathbf{T}_{\mathrm{v}}$ and $\mathbf{T}_{\mathrm{i}}$ are calculated through an eigenvalue/eigenvector problem such that the products $\mathbf{ZY}$ and $\mathbf{YZ}$ are diagonalized

$$\mathbf{T}_{\mathrm{v}}^{-1}\mathbf{ZYT}_{\mathrm{v}} = \mathbf{\Lambda} \tag{26a}$$

$$\mathbf{T}_{\mathrm{i}}^{-1}\mathbf{YZT}_{\mathrm{i}} = \mathbf{\Lambda} \tag{26b}$$

being $\mathbf{\Lambda}$ a diagonal matrix.

Thus, the line equations in modal quantities become:

$$-\frac{d\mathbf{V}_{\mathrm{m}}}{dx} = \mathbf{T}_{\mathrm{v}}^{-1}\mathbf{ZT}_{\mathrm{i}}\mathbf{I}_{\mathrm{m}} \tag{27a}$$

$$-\frac{d\mathbf{I}_{\mathrm{m}}}{dx} = \mathbf{T}_{\mathrm{i}}^{-1}\mathbf{YT}_{\mathrm{v}}\mathbf{V}_{\mathrm{m}} \tag{27b}$$

On transposing (26a) and comparing it with (26b) it follows that $\mathbf{T}_{\mathrm{v}}$ and $\mathbf{T}_{\mathrm{i}}$ can be chosen in a way that $\left[\mathbf{T}_{\mathrm{v}}\right]^{-1} = \left[\mathbf{T}_{\mathrm{i}}\right]^{\mathrm{T}}$ and the products $\mathbf{T}_{\mathrm{v}}^{-1}\mathbf{ZYT}_{\mathrm{i}}$ $(= \mathbf{Z}_{\mathrm{m}})$ and $\mathbf{T}_{\mathrm{i}}^{-1}\mathbf{YT}_{\mathrm{v}}$ $(= \mathbf{Y}_{\mathrm{m}})$ are diagonal (Dommel, 1986). Superscript T denotes transposed.

The solution of a line in modal quantities can be then expressed in a similar manner as in Eqs. (23). The solution in time domain is obtained again by using convolution, as in Eqs. (24). However, since both $\mathbf{T}_{\mathrm{v}}$ and $\mathbf{T}_{\mathrm{i}}$ are frequency dependent, a new convolution is needed to obtain line variables in phase quantities:

$$\mathbf{v}_{\mathrm{ph}}(t) = \mathbf{t}_{\mathrm{v}}(t) * \mathbf{v}_{\mathrm{m}}(t) \tag{28a}$$

$$\mathbf{i}_{\mathrm{ph}}(t) = \mathbf{t}_{\mathrm{i}}(t) * \mathbf{i}_{\mathrm{m}}(t) \tag{28b}$$

The procedure to solve the equations of a multi-conductor frequency-dependent overhead line in the time domain involves in each time step the following:

1) Transformation from phase-domain terminal voltages to modal domain.
2) Solution of the line equations using modal quantities, and calculation of (past history) current sources.
3) Transformation of current sources to phase-domain quantities.

Figure 7 shows a schematic diagram of the solution of overhead line equations in the modal domain.

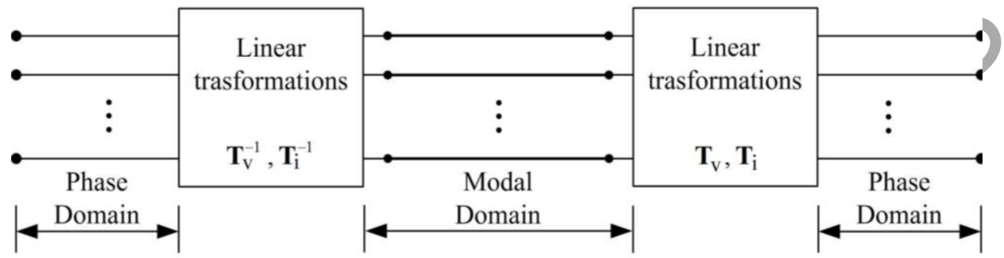

Figure 7. Transformations between phase domain and modal domain quantities.

Two approaches have been used for the solution of the line equations in modal quantities: constant and frequency-dependent transformation matrices.

a) The modal decomposition is made by using a constant real transformation matrix $\mathbf{T}$ calculated at a user-specified frequency, being the imaginary part usually discarded. This has been the traditional approach for many years. It has an obvious advantage, as it simplifies the problem of passing from modal quantities to phase quantities and reduces the number of convolutions to be calculated in the time domain, since $\mathbf{T}_{\mathrm{v}}$ and $\mathbf{T}_{\mathrm{i}}$ are real and constant. Differences between methods in the time-domain implementation, based on this approach, differ from the way in which the characteristic admittance function $\mathbf{Y}_{\mathrm{c}}$ and the propagation function $\mathbf{H}$ of each mode are represented. The characteristic admittance function is in general very smooth and can be easily synthesized with RC networks. To evaluate the convolution that involves the propagation function, several alternatives have been proposed: weighting functions (Meyer & Dommel, 1974), exponential recursive convolution (Semlyen & Dabuleanu, 1975), linear recursive convolution (Ametani, 1976), and modified recursive convolution (Marti, 1982).
b) The frequency dependence of the modal transformation matrix can be very significant for some untransposed multi-circuit lines. An accurate time-domain solution using a modal-domain technique requires then frequency-dependent transformation matrices. This can, in principle, be achieved by carrying out the transformation between modal- and phase-domain quantities as a time-domain convolution, with modal parameters and transformation matrix elements fitted with rational functions (Marti, 1988; Wedepohl, Nguyen, & Irwin, 1996). Although

working for cables, it has been found that for overhead lines, the elements of the transformation matrix cannot be always accurately fitted with stable poles only (Gustavsen & Semlyen, 1998a). This problem is overcome by the phase-domain approaches.

2.4.3. Phase-domain Solution Techniques

Some problems associated with frequency-dependent transformation matrices could be avoided by performing the transient calculation of an overhead line directly with phase quantities. A summary of the main approaches is presented below.

a) *Phase-domain numerical convolution*: Initial phase-domain techniques were based on a direct numerical convolution in the time domain (Nakanishi & Ametani, 1986). However, these approaches are time consuming in simulations involving many time steps. This drawback was partially solved by Gustavsen, Sletbak, & Henriksen (1995) by applying linear recursive convolution to the tail portion of the impulse responses.

b) *z-domain approaches*: An efficient approach is based on the use of two-sided recursions (TSR), as presented by Angelidis & Semlyen (1995). The basic input-output in the frequency domain is usually expressed as follows:

$$\mathbf{y}(s) = \mathbf{H}(s)\mathbf{u}(s) \tag{29}$$

Taking into account the rational approximation of $\mathbf{H}(s)$, Eq. (29) becomes:

$$\mathbf{y}(s) = \mathbf{D}^{-1}(s)\mathbf{N}(s)\mathbf{u}(s) \tag{30}$$

being $\mathbf{D}(s)$ and $\mathbf{N}(s)$ polynomial matrices. From this equation one can obtain:

$$\mathbf{D}(s)\mathbf{y}(s) = \mathbf{N}(s)\mathbf{u}(s) \tag{31}$$

This relation can be solved in the time domain using two convolutions:

$$\sum_{k=0}^{n} D_k y_{r-k} = \sum_{k=0}^{n} N_k u_{r-k} \tag{32}$$

The identification of both side coefficients can be made using a frequency-domain fitting. A more powerful implementation of the TSR, known as ARMA (Auto-Regressive Moving Average) model, was presented by Noda, Nagaoka, & Ametani (1996, 1997) by explicitly introducing modal time delays in (32).

c) *s-domain approaches*: A third approach is based on *s*-domain fitting with rational functions and recursive convolutions in the time domain. Two main aspects are issued: how to obtain the symmetric admittance matrix, $\mathbf{Y}$, and how to update the current source vectors. These tasks imply the fitting of $\mathbf{Y}_c(\omega)$ and $\mathbf{H}(\omega)$. The elements of $\mathbf{Y}_c(\omega)$ are smooth functions and can be easily fitted. However, the fitting of $\mathbf{H}(\omega)$ is more difficult since its elements may contain different time delays from individual modal contributions; in particular, the time delay of the ground mode differs from those of the aerial modes. Some works consider a single time delay for each element of $\mathbf{H}(\omega)$ (Nguyen, Dommel, & Marti, 1997). However, a very high order fitting can be necessary for the propagation matrix in the case of lines with a high ground resistivity, as an oscillating behavior can result in the frequency domain due to the uncompensated parts of the time delays. This problem can be solved by including modal time delays in the phase domain. Several line models have been developed on this basis, using polar decomposition (Gustavsen & Semlyen, 1998c), expanding $\mathbf{H}(\omega)$ as a linear combination of the modal propagation functions with idempotent coefficient matrices (Castellanos, Marti, & Marcano, 1997), or calculating unknown residues once the poles and time delays have been pre-calculated from the modal functions in the *universal line model* (Morched, Gustavsen, & Tartibi, 1999).

d) *Non-homogeneous models*: The series impedance matrix $\mathbf{Z}$ can be split up as:

$$\mathbf{Z}(\omega) = \mathbf{Z}_{\text{loss}}(\omega) + j\omega\mathbf{L}_{\text{ext}} \tag{33}$$

where

$$\mathbf{Z}_{\text{loss}}(\omega) = \mathbf{R} + j\omega\Delta\mathbf{L} \tag{34}$$

Elements of $\mathbf{L}_{\text{ext}}$ are frequency independent and related to the external flux, while elements of $\mathbf{R}$ and $\Delta\mathbf{L}$ are frequency dependent and related to the internal flux. Finally, the elements of the shunt admittance matrix, $\mathbf{Y}(\omega) = j\omega\mathbf{C}$, depend on the capacitances, which can be assumed frequency independent. Taking into account this behavior, frequency-dependent effects can be separated, and a line section can be represented as shown in Figure 8 (Castellanos & Marti, 1997).

Modeling $\mathbf{Z}_{\text{loss}}$ as lumped has advantages, since their elements can be synthesized in phase quantities, and limitations, since a line has to be divided into sections to reproduce the distributed nature of parameters.

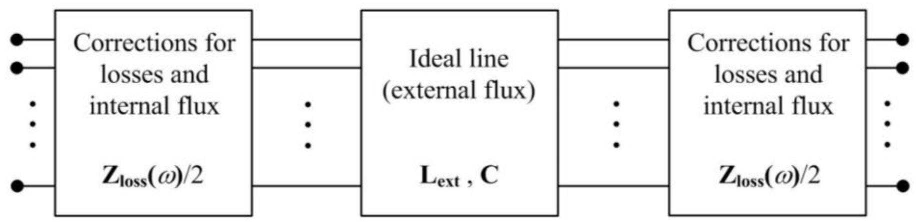

Figure 8. Section of a non-homogeneous line model.

2.4.4. Alternate Solution Techniques

Other techniques used to solve line equations use *finite differences models*. In this type of models the set of partial differential Eqs. (1) are converted to an equivalent set of ordinary differential equations. This new set is discretized with respect to the distance and time by finite differences and solved sequentially along the time (Naredo, Soudack, & Martí, 1995). It has been shown that these models have advantages over those described above when the line has to be discretized, for instance in the presence of incident external fields and/or corona effect (Ramírez, Naredo, & Moreno, 2005).

2.5. Data Input and Output. Line Constants Routine

Users of EMT programs obtain overhead line parameters by means of a dedicated supporting routine which is usually denoted “Line Constants” (LC) (Dommel, 1986). In addition, several routines are presently implemented in transients programs to create line models considering different approaches (Marti, 1982; Noda, Nagaoka, & Ametani, 1996; Morched, Gustavsen, & Tartibi, 1999). This section describes the most basic input requirements of LC-type routines.

LC routine users enter the physical parameters of the line and select the desired type of line model. This routine allows users to request the following models:

- lumped-parameter equivalent or nominal pi-circuits, at the specified frequency;
- constant distributed-parameter model, at the specified frequency;
- frequency-dependent distributed-parameter model, fitted for a given frequency range.

In order to develop line models for transient simulations, the following input data must be available:

- (x, y) coordinates and radii of each conductor and shield wire;
- bundle spacing, orientations;
- sag of phase conductors and shield wires;
- phase and circuit designation of each conductor;
- phase rotation at transposition structures;
- physical dimensions of each conductor;
- DC resistance of each conductor and shield wire (or resistivity);
- ground resistivity of the ground return path.

Other information such as segmented ground wires can be important.

Note that all the above information, except conductor resistances and ground resistivity, comes from the transversal line geometry.

The following information can be usually provided by the routine:

- the capacitance or the susceptance matrix;
- the series impedance matrix;
- resistance, inductance and capacitance per unit length for zero and positive sequences, at a given frequency or for a specified frequency range;
- surge impedance, attenuation, propagation velocity and wavelength for zero and positive sequences, at a given frequency or for a specified frequency range.

Line matrices can be provided for the system of physical conductors, the system of equivalent phase conductors, or symmetrical components of the equivalent phase conductors. Notice however that the use of sequence parameters and symmetrical components involves the underlying assumption of lines being perfectly balanced or continuously transposed.

3. Insulated Cables

3.1. Introduction

The electromagnetic behavior of a transmission cable also is described by Eqs. (1a) and (1b) as for an overhead line (Dommel, 1986; Wedepohl & Wilcox, 1973; Ametani, 1980b). The difference is in the calculation of parameters:

$$\mathbf{Z}(\omega) = \mathbf{R}(\omega) + j\omega\mathbf{L}(\omega) \qquad (35a)$$
$$\mathbf{Y}(\omega) = \mathbf{G}(\omega) + j\omega\mathbf{C}(\omega) \qquad (35b)$$

where $\mathbf{R}$, $\mathbf{L}$, $\mathbf{G}$ and $\mathbf{C}$ are the cable parameter matrices expressed in per unit length. These quantities are $(n \times n)$ matrices, being n the number of (parallel) conductors of the cable system. The variable ω stresses the fact that these quantities are calculated as function of frequency.

As for overhead lines, most EMT tools have dedicated supporting routines for the calculation of cable parameters. These routines have very similar features, and hereinafter they will be given the generic name "Cable Constants" (CC).

Guidelines for representing insulated cables in EMT studies are similar to those proposed for overhead lines (see Section 2.1 and Table 3). In addition, the solution of cable equations can be carried out following the same techniques proposed in the previous section. However, the large variety of cable designs makes very difficult the development of a single computer routine for calculating the parameter of each design.

The calculation of matrices $\mathbf{Z}$ and $\mathbf{Y}$ uses cable geometry and material properties as input parameters. In general, CC users must specify:

1. *Geometry*: location of each conductor ($x-y$ coordinates); inner and outer radii of each conductor; burial depth of the cable system.
2. *Material properties*: resistivity, ρ, and relative permeability, μ_r, of all conductors (μ_r is unity for all non-magnetic materials); resistivity and relative permeability of the surrounding medium, ρ, μ_r; relative permittivity of each insulating material, ε_r.

Accurate input data are in general more difficult to obtain for cable systems than for overhead lines as the small geometrical distances make the cable parameters highly sensitive to errors in the specified geometry. In addition, it is not straightforward to represent certain features such as wire screens, semiconducting screens, armors, and lossy insulation materials. It is worth noting that CC routines take the skin effect into account but neglect proximity effects. Besides these routines have some shortcomings in representing certain cable features.

A previous conversion procedure may be required in order to bring the available cable data into a form which can be used as input to a CC routine. This conversion is frequently needed because input cable data can have alternative representations, while CC routines only support one representation and they do not consider certain cable features, such as semi-conducting screens and wire screens.

The following subsections of this chapter introduce the main cable designs for high voltage applications, summarize the calculation of cable parameters for EMT studies, and suggest a procedure for preparing the input data of a cable whose design cannot be directly specified in a CC routine.

3.2. Insulated cable designs

3.2.1. Single core self-contained cables

They are coaxial in nature, see Figure 9. The insulation system can be based on extruded insulation (e.g., XLPE) or oil-impregnated paper (fluid-filled or mass-impregnated). The core conductor can be hollow in the case of fluid-filled cables.

Self-contained (SC) cables for high-voltage applications are always designed with a metallic sheath conductor, which can be made of lead, corrugated aluminum, or copper wires. Such cables are also designed with an inner and an outer semiconducting screen, which are in contact with the core conductor and the sheath conductor, respectively.

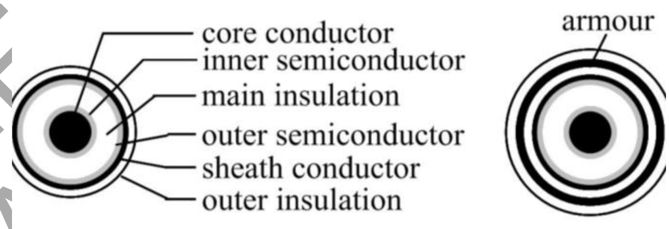

Figure 9. SC XLPE cable, with and without armor.

3.2.2. Three-phase Self-contained Cables

They consist of three SC cables which are contained in a common shell. The insulation system of each SC cable can be based on extruded insulation or on paper-oil. Most designs can be differentiated into the two designs shown in Figure 10:

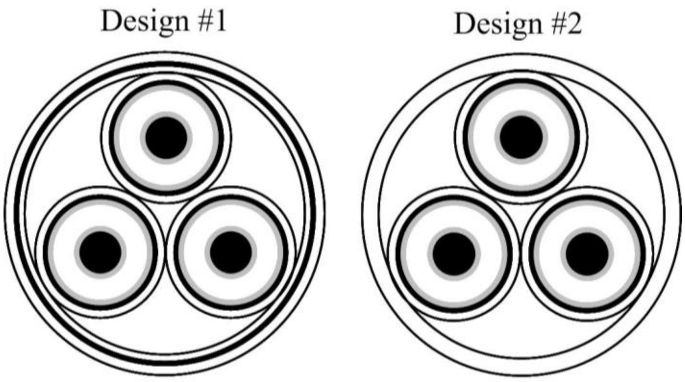

Figure 10. Three-phase cable designs.

- Design #1: One metallic sheath for each SC cable, with cables enclosed within metallic pipe (sheath/armor). This design can be directly modeled using the "pipe-type" representation available in some CC routines.
- Design #2: One metallic sheath for each SC cable, with cables enclosed within insulating pipe. None of the present CC routines can directly deal with this type of design due to the common *insulating* enclosure. This limitation can be overcome in one of the following ways:
    a) Place a very thin conductive conductor on the inside of the insulating pipe. The cable can then be represented as a pipe-type cable in a CC routine.
    b) Place the three SC cables directly in earth (and ignore the insulating pipe).

  Both options should give reasonably accurate results when the sheath conductors are grounded at both ends. However, these approaches are not valid when calculating induced sheath overvoltages.

The space between the SC cables and the enclosing pipe is for both designs filled by a composition of insulating materials; however, CC routines only permit to specify a homogenous material between sheaths and the metallic pipe.

3.2.3. Pipe-type Cables

They consist of three SC paper cables that are laid asymmetrically within a steel pipe, which is filled with pressurized low viscosity oil or gas, see Figure 11. Each SC cable is fitted with a metallic sheath. The sheaths may be touching each other.

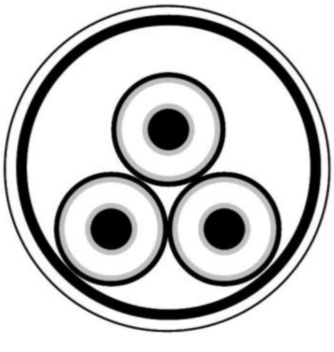

Figure 11. Pipe type cable.

3.3. Material Properties

Table 4 shows appropriate values for common materials used in insulated cable designs (Gustavsen, Noda, Naredo, Uribe, Martinez-Velasco, 2009).

Cable section	Property	Material and values	
Conductors	Resistivity (Ω.m)	Copper	1.72*E*-8
		Aluminium	2.83*E*-8
		Lead	22*E*-8
		Steel	18*E*-8
Insulation layers	Relative permittivity	XLPE	2.3
		Mass-impregnated	4.2
		Fluid-filled	3.5
Semiconducting layers	Resistivity (Ω.m)	< 1*E*-3	
	Relative permittivity	> 1000	

Table 4. Resistivity of conductive materials

Conductors: Stranded conductors need to be modeled as massive conductors. The resistivity should be increased with the inverse of the fill factor of the conductor surface so as to give the correct resistance of the conductor. The resistivity of the surrounding ground depends strongly on the soil characteristics, ranging from about 1 Ω.m (wet soil) to about 10 kΩ.m (rock). The resistivity of sea water lies between 0.1 and 1 Ω.m.

Insulations: The relative permittivity of the main insulation is usually obtained from the manufacturer. The values shown in Table 4 were measured at power frequency. Most extruded insulations, including XLPE and PE, are practically lossless up to 1 MHz, whereas paper-oil type insulations exhibit significant losses also at lower frequencies. The losses are associated with a permittivity that is complex and frequency-dependent:

$$\varepsilon_{\mathrm{r}}(\omega) = \varepsilon'_{\mathrm{r}}(\omega) - j\varepsilon''_{\mathrm{r}}(\omega) \qquad \tan\delta(\omega) = \frac{\varepsilon''_{\mathrm{r}}}{\varepsilon'_{\mathrm{r}}} \tag{36}$$

where $\tan\delta$ is the insulation loss factor.

At present, CC routines do not allow to enter a frequency-dependent loss factor, so a constant value has to be specified. However, this could lead to non-physical frequency responses which cannot be accurately fitted by frequency-dependent transmission line models. Therefore, the loss-angle should instead be specified as zero.

Breien & Johansen (1971) fitted the measured frequency response of insulation samples of a low-pressure fluid-filled cable in the frequency range 10 kHz – 100 MHz. The permittivity is given as:

$$\varepsilon_{\mathrm{r}} = 2.5 + \frac{0.94}{1+\left(j\omega 6\times 10^{-9}\right)^{0.315}} \tag{37}$$

The permittivity at zero frequency is real-valued and equal to 3.44. According to Breien & Johansen (1971), the frequency-dependent permittivity causes additional attenuation of pulses shorter than 5 μs.

Semiconducting materials: The main insulation of high-voltage cables for both extruded insulation and paper-oil insulation is always sandwiched between two semiconducting layers. The electric parameters of semiconducting screens can vary between wide limits. The values shown in Table 4 are indicative values for extruded insulation. The resistivity is required by norm to be smaller than 1*E*-3 Ω.m. Semiconducting layers can in most cases be taken into account by using a simplistic approach that is explained later on at Sections 3.5.

3.4. Calculation of Cable Parameters

This section focuses mostly on coaxial configurations. Other transversal geometries should be approximated to this or dealt with through auxiliary methods such as those based on Finite Element Analysis (Yin & Dommel, 1989) or on subdivision of conductors (Zhou & Marti, 1994).

3.4.1. Coaxial Cables

The calculation of the elements of both the series impedance matrix and the shunt capacitance matrix is presented below.

Series impedance matrix: The series impedance matrix of a coaxial cable can be obtained by means of a two-step procedure. First, surface and transfer impedances of a hollow conductor are derived; then they are rearranged into the form of the series impedance matrix that can be used for describing traveling-wave propagation (Schelkunoff, 1934; Rivas & Marti, 2002). Figure 12 shows the cross section of a coaxial cable with the three conductors (i.e., *core*, *metallic sheath*, and *armor*) and the currents flowing down each one. Some coaxial cables do not have armor. Insulations A and B are sometimes called *bedding* and *plastic sheath*, respectively (Dommel, 1986).

Consider a hollow conductor whose inner and outer radii are a and b respectively. Figure 13 shows its cross section. The inner surface impedance Z_{aa} and the outer surface impedance Z_{bb}, both in per unit length (p.u.l.), are given by Schelkunoff (1934):

$$Z_{aa} = \frac{\rho m}{2\pi a}\frac{I_0(ma)K_1(mb)+I_1(mb)K_0(ma)}{I_1(mb)K_1(ma)-I_1(ma)K_1(mb)} \tag{38a}$$

$$Z_{bb} = \frac{\rho m}{2\pi b}\frac{I_0(mb)K_1(ma)+I_1(ma)K_0(mb)}{I_1(mb)K_1(ma)-I_1(ma)K_1(mb)} \tag{38b}$$

where

$$m = \sqrt{j\omega \frac{\mu}{\rho}} \tag{39}$$

being ρ and μ the resistivity and the permeability of the conductor, respectively. $I_n(.)$ and $K_n(.)$ are the *n*-th order Modified Bessel Functions of the first and the second kind, respectively.

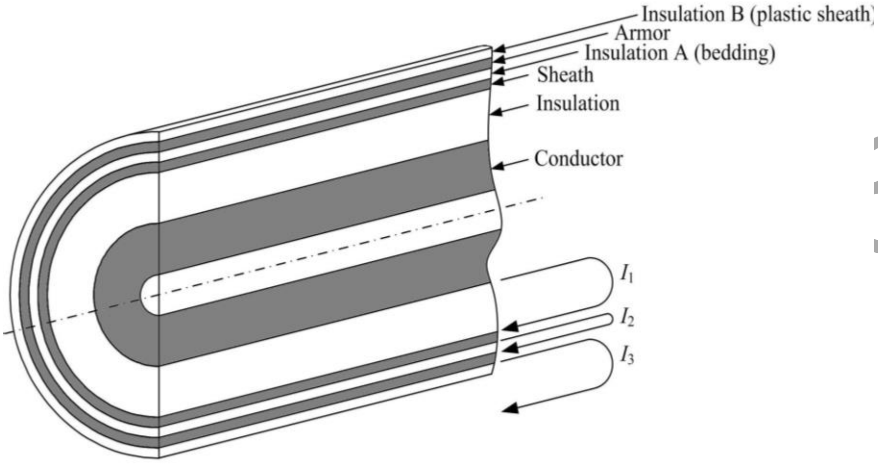

Figure 12. Cross section of a coaxial cable.

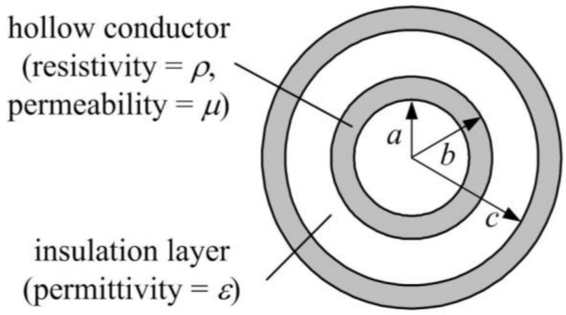

Figure 13. Cross section of a coaxial cable with a hollow conductor.

Z_{aa} can be seen as the p.u.l. impedance of the hollow conductor for the current returning inside the conductor, while Z_{bb} is the p.u.l. impedance for the current returning outside the conductor.

The p.u.l. transfer impedance Z_{ab} from one surface to the other is calculated as follows (Schelkunoff, 1934):

$$Z_{ab} = \frac{\rho}{2\pi ab} \frac{1}{I_1(mb)K_1(ma) - I_1(ma)K_1(mb)} \tag{40}$$

The impedance of an insulating layer between two hollow conductors, whose inner and outer radii are respectively b and c, see Figure 13, is given by the following expression:

$$Z_i = j\omega \frac{\mu}{2\pi} \ln \frac{c}{b} \tag{41}$$

where μ is the permeability of the insulation.

The ground-return impedance of an underground wire can be calculated by means of the following general expression (Pollaczek, 1926; Pollaczek, 1927):

$$Z_g = \frac{\rho m^2}{2\pi} \left[K_0(mD_1) - K_0(mD_2) + \int_{-\infty}^{+\infty} \frac{\mathrm{e}^{-Y\sqrt{\lambda^2+m^2}}}{|\lambda| + \sqrt{\lambda^2+m^2}} \mathrm{e}^{j\lambda x} d\lambda \right] \tag{42}$$

where m is given by (39) and ρ is the ground resistivity.

The p.u.l. self impedance of a wire placed at a depth of y with radius r is obtained by substituting

$$D_1 = r \qquad D_2 = \sqrt{r^2 + 4y^2} \tag{43}$$

into (42).

To obtain the p.u.l. mutual impedance of two wires, placed at depths of y_i and y_j with horizontal separation $(x_i - x_j)$, substitute

$$D_1 = \sqrt{(x_i - x_j)^2 + (y_i - y_j)^2} \qquad D_2 = \sqrt{(x_i - x_j)^2 + (y_i + y_j)^2} \tag{44}$$

into (42).

Consider the coaxial cable shown in Figure 12. Assume that I_1 is the current flowing down the core and returning through the sheath, I_2 flows down the sheath and returns through the armor, and I_3 flows down on the armor and its return path is the external ground soil, see Figure 12. If V_1, V_2, and V_3 are the voltage differences between the core and the sheath, between the sheath and the armor, and between the armor and the ground, respectively, the relationships between currents and voltages can be expressed as follows (Dommel, 1986):

$$-\frac{\partial}{\partial x}\begin{bmatrix} V_1 \\ V_2 \\ V_3 \end{bmatrix} = \begin{bmatrix} Z_{11} & Z_{12} & 0 \\ Z_{21} & Z_{22} & Z_{23} \\ 0 & Z_{23} & Z_{33} \end{bmatrix}\begin{bmatrix} I_1 \\ I_2 \\ I_3 \end{bmatrix} \tag{45}$$

where

$$\begin{aligned} Z_{11} &= Z_{bb(\text{core})} + Z_{i(\text{core-sheath})} + Z_{aa(\text{sheath})} \\ Z_{22} &= Z_{bb(\text{sheath})} + Z_{i(\text{sheath-armor})} + Z_{aa(\text{armor})} \\ Z_{33} &= Z_{bb(\text{armor})} + Z_{i(\text{armor-ground})} + Z_{\text{g}} \\ Z_{12} &= -Z_{ab(\text{sheath})} \\ Z_{23} &= -Z_{ab(\text{armor})} \end{aligned} \tag{46}$$

$Z_{aa(\text{conductor})}$, $Z_{bb(\text{conductor})}$ and $Z_{ab(\text{conductor})}$ are calculated by substituting the inner and outer radii of the conductor into (38a), (38b) and (40); $Z_{i(\text{insulator})}$ is calculated by substituting the inner and outer radii of the designated insulator layer into (41); Z_g is the self ground-return impedance of the armor obtained from (42).

An algebraic manipulation of (45) using the following relationships:

$$\begin{aligned} V_1 &= V_{\text{core}} - V_{\text{sheath}} & I_1 &= I_{\text{core}} \\ V_2 &= V_{\text{sheath}} - V_{\text{armor}} & I_2 &= I_{\text{core}} + I_{\text{sheath}} \\ V_3 &= V_{\text{armor}} & I_3 &= I_{\text{core}} + I_{\text{sheath}} + I_{\text{armor}} \end{aligned} \tag{47}$$

gives

$$-\frac{\partial}{\partial x}\begin{bmatrix} V_{\text{core}} \\ V_{\text{sheath}} \\ V_{\text{armor}} \end{bmatrix} = Z_{3\times 3}\begin{bmatrix} I_{\text{core}} \\ I_{\text{sheath}} \\ I_{\text{armor}} \end{bmatrix} \tag{48}$$

where $\mathbf{Z}_{3\times 3}$ is the p.u.l. series impedance matrix of the coaxial cable shown in Figure 12 when a single coaxial cable is buried alone.

When more than two parallel coaxial cables are buried together, mutual couplings among the cables must be accounted for. The three-phase case is illustrated in the following paragraph. Among the circulating currents I_1, I_2 and I_3, only I_3 has mutual couplings between different cables. Using subscripts a, b and c to denote the phases of the three cables, Eq. (45) can be expanded into the following form (Dommel, 1986):

$$-\frac{\partial}{\partial x}\begin{bmatrix}\mathbf{V}_{\mathrm{a}}\\ \mathbf{V}_{\mathrm{b}}\\ \mathbf{V}_{\mathrm{c}}\end{bmatrix}=\begin{bmatrix}\mathbf{Z}_{\mathrm{a}} & \mathbf{Z}_{\mathrm{g,ab}} & \mathbf{Z}_{\mathrm{g,ac}}\\ \mathbf{Z}_{\mathrm{g,ba}} & \mathbf{Z}_{\mathrm{b}} & \mathbf{Z}_{\mathrm{g,bc}}\\ \mathbf{Z}_{\mathrm{g,ca}} & \mathbf{Z}_{\mathrm{g,cb}} & \mathbf{Z}_{\mathrm{c}}\end{bmatrix}\begin{bmatrix}\mathbf{I}_{\mathrm{a}}\\ \mathbf{I}_{\mathrm{b}}\\ \mathbf{I}_{\mathrm{c}}\end{bmatrix} \tag{49}$$

where

$$\mathbf{V}_i=\begin{bmatrix}V_{1i}\\ V_{2i}\\ V_{3i}\end{bmatrix}\quad \mathbf{I}_i=\begin{bmatrix}I_{1i}\\ I_{2i}\\ I_{3i}\end{bmatrix}\qquad i=\mathrm{a,\ b,\ c} \tag{50a}$$

$$\mathbf{Z}_i=\begin{bmatrix}Z_{11i} & Z_{12i} & 0\\ Z_{21i} & Z_{22i} & Z_{23i}\\ 0 & Z_{32i} & Z_{33i}\end{bmatrix}\qquad i=\mathrm{a,\ b,\ c} \tag{50b}$$

$$\mathbf{Z}_{g,ij}=\begin{bmatrix}0 & 0 & 0\\ 0 & 0 & 0\\ 0 & 0 & Z_{g,ij}\end{bmatrix}\qquad i,\ j=\mathrm{a,\ b,\ c} \tag{50c}$$

where $Z_{\mathrm{g,ab}}$ is the mutual ground-return impedance between the armors of the phases a and b; $Z_{\mathrm{g,bc}}$ and $Z_{\mathrm{g,ca}}$ are the mutual ground-return impedances between b and c and between c and a, respectively. These mutual ground-return impedances can be obtained from (42).

Using the relationship (47) for each phase, an algebraic manipulation leads to the following final form:

$$-\frac{\partial}{\partial x}\begin{bmatrix}V_{\mathrm{core,a}}\\ V_{\mathrm{sheath,a}}\\ V_{\mathrm{armor,a}}\\ V_{\mathrm{core,b}}\\ V_{\mathrm{sheath,b}}\\ V_{\mathrm{armor,b}}\\ V_{\mathrm{core,c}}\\ V_{\mathrm{sheath,c}}\\ V_{\mathrm{armor,c}}\end{bmatrix}=\mathbf{Z}_{9\times 9}\begin{bmatrix}I_{\mathrm{core,a}}\\ I_{\mathrm{sheath,a}}\\ I_{\mathrm{armor,a}}\\ I_{\mathrm{core,b}}\\ I_{\mathrm{sheath,b}}\\ I_{\mathrm{armor,b}}\\ I_{\mathrm{core,c}}\\ I_{\mathrm{sheath,c}}\\ V_{\mathrm{armor,c}}\end{bmatrix} \tag{51}$$

where $\mathbf{Z}_{9\times 9}$ is the p.u.l. series impedance matrix of the three-phase coaxial cable.
A general and systematic method to convert the loop impedance matrix of cables into their series impedance matrix has been developed by Noda (2008).

Shunt admittance matrix: The p.u.l. capacitance of the insulation layer between the two hollow conductors shown in Figure 13 is given by:

$$C_1 = \frac{2\pi\varepsilon}{\ln\frac{c}{b}} \tag{52}$$

where ε is the permittivity of the insulation layer and a, b, c are the radii as shown in Figure 13..

If the dielectric losses are ignored, the p.u.l. admittance is $Y_i = j\omega C_i$, and the relationship between currents and voltages can be expressed as follows:

$$-\frac{\partial}{\partial x}\begin{bmatrix} I_{\text{core}} \\ I_{\text{sheath}} \\ I_{\text{armor}} \end{bmatrix} = \mathbf{Y}_{3\times3}\begin{bmatrix} V_{\text{core}} \\ V_{\text{sheath}} \\ V_{\text{armor}} \end{bmatrix} \tag{53}$$

where

$$\mathbf{Y}_{3\times3} = \begin{bmatrix} Y_1 & -Y_1 & 0 \\ -Y_1 & Y_1 + Y_2 & -Y_2 \\ 0 & -Y_2 & Y_2 + Y_3 \end{bmatrix} \tag{54}$$

is the p.u.l. shunt admittance matrix of the coaxial cable shown in Figure 12 when a single coaxial cable is buried alone.

There are no electrostatic couplings between the cables, when more than two parallel coaxial cables are buried together. Thus, the p.u.l. shunt admittance matrix for a three-phase cable can be expressed as follows:

$$\mathbf{Y}_{9x9} = \begin{bmatrix} \mathbf{Y}_{\text{a}} & 0 & 0 \\ 0 & \mathbf{Y}_{\text{b}} & 0 \\ 0 & 0 & \mathbf{Y}_{\text{c}} \end{bmatrix} \tag{55}$$

where

$$\mathbf{Y}_i = \begin{bmatrix} Y_{1i} & -Y_{1i} & 0 \\ -Y_{1i} & Y_{1i} + Y_{2i} & -Y_{2i} \\ 0 & -Y_{2i} & Y_{2i} + Y_{3i} \end{bmatrix} \quad i = \text{a,b,c} \tag{56}$$

where the subscripts a, b and c denote the phases of the three cables. If the dielectric losses are considered, a real part is added to $\mathbf{Y}_i$, see (36).

3.4.2. Pipe-type Cables

The calculation of the series impedance matrix and the shunt capacitance matrix is presented in the following paragraphs.

Series impedance matrix: Since the penetration depth into the pipe at power frequency is usually smaller than the pipe thickness, it is reasonable to assume that the pipe is the only return path and the ground-return current can be ignored. In this case, an infinite pipe thickness can be assumed. A technique to account for the ground-return current was proposed by Ametani (1980b).

For each coaxial cable in the pipe, the impedance matrix for circulating currents given in (45) can be used. The matrix elements are calculated using the Eqs. (46), except that for Z_{33}, which is replaced by:

$$Z_{33} = Z_{bb(\text{armor})} + Z_{i(\text{armor-pipe})} + Z_{aa(\text{pipe})} \tag{57}$$

where $Z_{bb(\text{armor})}$ is obtained from (38b).

Since the conductor geometry of a pipe-type cable is not concentric with respect to the pipe centre, the formula for $Z_{i(\text{armor-pipe})}$ is somewhat complicated compared with (41):

$$Z_{i(\text{armor-pipe})} = j\omega \frac{\mu}{2\pi} \ln\left[\frac{R}{r} \left\{ 1 - \left(\frac{d}{R} \right)^2 \right\} \right] \tag{58}$$

where μ is the permeability of the insulation between the armor and the pipe, R is the radius of the pipe, r is the radius of the armor of interest, d is the offset of the coaxial cable of interest from the pipe centre.

On the other hand, $Z_{aa(\text{pipe})}$ is calculated as follows:

$$Z_{aa(\text{pipe})} = j\omega \frac{\mu}{2\pi} \left[\frac{K_0(mR)}{mRK_1(mR)} + 2\sum_{n=1}^{\infty} \left(\frac{d}{R} \right)^{2n} \frac{K_n(mR)}{n\mu_r K_n(mR) - mRK_n'(mR)} \right] \tag{59}$$

where m is given in (39), $\mu = \mu_0 \mu_\text{r}$ is the permeability of the pipe, and $K_n'(.)$ is the derivative of $K_n(.)$.

To take into account the mutual impedance among the coaxial cables in a pipe, the impedance matrix for circulating currents given in (51) has to be built. Since an infinite pipe thickness is assumed, $Z_{\text{g,ab}}$, $Z_{\text{g,bc}}$ and $Z_{\text{g,ca}}$ are replaced by $Z_{\text{p,ab}}$, $Z_{\text{p,bc}}$ and $Z_{\text{p,ca}}$ (the subscript p designates pipe) and they are deduced by substituting the phase indexes a, b, and c into i and j in the following expression:

$$Z_{\mathrm{p},ij} = j\omega \frac{\mu}{2\pi}\left[\ln \frac{R}{\sqrt{d_i^2 + d_j^2 - 2d_i d_j \cos\theta_{ij}}} + \mu_\mathrm{r} \frac{K_0(mR)}{mRK_1(mR)} + \sum_{n=1}^{\infty}\left(\frac{d_i d_j}{R^2}\right)^n \cos(n\theta_{ij})\left\{2\mu_\mathrm{r} \frac{K_n(mR)}{n\mu_\mathrm{r}K_n(mR) - mRK_n'(mR)} - \frac{1}{n}\right\}\right] \tag{60}$$

where d_i is the offset of the *i*-phase coaxial cable from the pipe centre, d_j is the offset of the *j*-phase coaxial cable from the pipe centre, and θ_{ij} is the angle that the *i*-phase and the *j*-phase cables make with respect to the pipe centre.

The expressions (58), (59) and (60) are by Brown & Rocamora (1976). A method to take into account the saturation effect of a pipe wall was presented by Dugan, Brown & Rocamora (1977).

Shunt admittance matrix: The inverse of $\mathbf{Y}_{3\times3}$ in (54) multiplied by $j\omega$ gives the p.u.l. potential coefficient matrix of each coaxial cable in the pipe. If potential coefficients of phases a, b, and c are denoted as $\mathbf{P}_\mathrm{a}$, $\mathbf{P}_\mathrm{b}$, and $\mathbf{P}_\mathrm{c}$, the potential coefficient matrix of the whole cable system, including the pipe, is written in the form:

$$\mathbf{P}_{9x9} = \begin{bmatrix} \mathbf{P}_\mathrm{a} + \mathbf{P}_\mathrm{aa} & \mathbf{P}_\mathrm{ab} & \mathbf{P}_\mathrm{ac} \\ \mathbf{P}_\mathrm{ab} & \mathbf{P}_\mathrm{b} + \mathbf{P}_\mathrm{bb} & \mathbf{P}_\mathrm{bc} \\ \mathbf{P}_\mathrm{ca} & \mathbf{P}_\mathrm{cb} & \mathbf{P}_\mathrm{c} + \mathbf{P}_\mathrm{cc} \end{bmatrix} \tag{61}$$

where the submatrices $\mathbf{P}_\mathrm{ab}$, $\mathbf{P}_\mathrm{bb}$, and $\mathbf{P}_\mathrm{ca}$ consists of 9 identical elements which can be calculated by substituting the phase indexes a, b, and c into i and j in the following formulas (Brown & Rocamora, 1976):

$$P_{ii} = \frac{1}{2\pi\varepsilon}\ln\left[\frac{R}{r_i}\left\{1 - \left(\frac{d_i}{R}\right)^2\right\}\right] \tag{62a}$$

$$P_{ij} = \frac{1}{2\pi\varepsilon}\ln\frac{R}{\sqrt{d_i^2 + d_j^2 - 2d_i d_j \cos\theta_{ij}}} \tag{62b}$$

where ε is the permittivity of the insulation between the armors and the pipe.

Finally, the p.u.l. shunt admittance matrix is calculated as follows:

$$\mathbf{Y}_{9\times9} = j\omega\mathbf{P}_{9\times9}^{-1} \tag{63}$$

-

-

-

Bibliography

Abeywickrama K.G.N.B., Serdyuk Y.V., Gubanski S.M. (2006). Exploring possibilities for characterization of power transformer insulation by frequency response analysis (FRA), *IEEE Trans. on Power Delivery* 21, 1375-1382. [This paper explores the possibility for using frequency response analysis (FRA) technique to characterize the quality of transformer insulation].

Adjaye R.E., Cornick K.J. (1979). Distribution of switching surges in the line-end coils of cable-connected motors, *Electric Power Applications* 2, 11-21. [This paper presents several studies describing the interturn voltages in the line-end coils of cable-connected machines].

AlFuhaid A.S. (2001). Frequency characteristics of single phase two winding transformer using distributed parameter modeling, *IEEE Trans. on Power Delivery* 16, 637-642. [This paper uses modal analysis and modeling results from transmission-line theory in order to obtain the frequency characteristics of the transformer input impedance under different loading conditions, which can be useful in identifying the resonant frequencies of the transformer].

Aliprantis D.C., Sudhoff S.D., Kuhn B.T. (2005). Experimental characterization procedure for a synchronous machine model with saturation and arbitrary rotor network representation, *IEEE Trans. on Energy Conversion*, 20 595-603. [This paper describes the experimental procedure for determining the saturation characteristics of a salient pole synchronous machine, as well as other parameters that are used in the rotor model].

Ametani A. (1976). A highly efficient method for calculating transmission line transients, *IEEE Trans. on Power Apparatus Systems* 95, 1545-1551. [This paper presents a highly efficient method for digital calculation of transients on transmission lines with frequency-dependent effects].

Ametani A. (1980a). Wave propagation characteristics of cables, *IEEE Trans. on Power Apparatus and Systems* 99, 499-505. [This paper presents wave propagation characteristics of a single-core coaxial cable and a pipe enclosed cable].

Ametani. A. (1980b). A general formulation of impedance and admittance of cables, *IEEE Trans. on Power Apparatus and Systems* 99, 902-909. [This paper describes a general formulation of impedances and admittances of single-core coaxial and pipe-type cables].

Ametani A., Miyamoto Y., Nagaoka N. (2004). Semiconducting layer impedance and its effect on cable wave-propagation and transient characteristics, *IEEE Trans. on Power Delivery* 19, 1523-1531. [This paper proposes an impedance formula for semiconducting layers based on a conventional circuit theory].

Angelidis G., Semlyen A. (1995). Direct phase-domain calculation of transmission line transients using two-sided recursions, *IEEE Trans. on Power Delivery* 10, 941-949. [This paper presents a new method for the simulation of electromagnetic transients on transmission lines, which instead of using convolutions of the input variables only, it performs short convolutions with both input and output variables].

Arturi C.M. (1991). Transient simulation and analysis of a three-phase five-limb step-up transformer following an out-of-phase synchronization, *IEEE Trans. on Power Delivery* 6, 196-207. [This paper presents theoretical and experimental analyses of the electromagnetic transient following the out-of-phase synchronization of a three-phase five-limb step-up transformer, and also reports the results of an experimental validation made on a specially built 100 kVA three-phase five-limb transformer].

Avila-Rosales J., Alvarado F.L. (1982). Nonlinear frequency dependent transformer model for electromagnetic transient studies in power systems, *IEEE Trans. Power Apparatus and Systems* 101, 4281-4288. [This paper presents a procedure for taking into account the frequency dependent characteristics of the transformer based on an analysis of the electromagnetic field distribution within the laminations of the transformer core].

Bacvarov D.C., Sarma D.K. (1986). Risk of winding insulation breakdown in large ac motors caused by steep switching surges. Part I: Computed switching surges, *IEEE Trans. on Energy Conversion* 1, 130-139. [This paper demonstrates the applicability and use of the finite element method for probabilistic assessment of the risk of turn insulation breakdown in large AC motors].

Brandwajn V., Dommel H.W. (1976). Interfacing generator models with an electromagnetic transients program, *IEEE PES Summer Meeting*, Paper No. A76359-0, Portland. [This paper describes the methods of interfacing the synchronous machine model with the EMTP network using the Thevenin equivalent circuit that is derived from the discretized qd0 equivalent circuit. The proposed method requires prediction of electrical variables].

Brandwajn V. (1980). Representation of magnetic saturation in the synchronous machine model in an electro-magnetic transients program, *IEEE Trans. on Power Apparatus and Systems* 99, 1996-2002. [This paper describes the piece-wise linear representation of magnetic saturation of the synchronous machine model in EMTP, wherein the authors use two slope characteristic and define residual flux in order to formulate the linearized equations].

Brandwajn V., Dommel H.W., Dommel I.I. (1982). Matrix representation of three-phase n-winding transformers for steady-state and transient studies, *IEEE Trans. on Power Apparatus and Systems* 101, 1369-1378. [This paper describes the derivation of models for three-phase and single-phase N-winding transformers in the form of branch impedance or admittance matrices, which can be calculated from available test data of positive and zero sequence short-circuit and excitation tests].

Breien O., Johansen I. (1971). Attenuation of traveling waves in single-phase high-voltage cables, *Proc. IEE* 118, 787-793. [This paper calculates the attenuation due to the combined effect of dielectric losses in the cable insulation and the skin effect in the core and sheath].

Brown G.W., Rocamora R.G. (1976). Surge propagation in three-phase pipe-type cables, Part I – Unsaturated pipe, *IEEE Trans. on Power Apparatus and Systems* 95, 89-95. [This paper determines the step response of three-phase pipe-type cable, using solution techniques analogous to those developed by Carson for overhead transmission lines].

Cao X., Kurita A., Mitsuma H., Tada Y., Okamoto H. (1999). Improvements of numerical stability of electromagnetic transient simulation by use of phase-domain synchronous machine models, *Electrical Engineering in Japan* 128, 53-62. [This document describes the phenomena of poor numerical stability of the conventional qd models due to their interface and proposes to use the so-called phase-domain synchronous machine model to achieve direct interface of machine's electrical variables and the network and thus improve the numerical stability].

Carson J.R. (1926). Wave propagation in overhead wires with ground return, *Bell Syst. Tech. Journal* 5, 539-554. [This paper presents a solution to the problem of wave propagation along an overhead transmission wire parallel to ground and to the problem of inductive coupling with neighbor transmission wires when including the effect of the earth, which is represented as a homogeneous semi-infinite solid plane].

Castellanos F., Marti J.R. (1997). Full frequency-dependent phase-domain transmission line model, *IEEE Trans. on Power Systems* 12, 1331-1339. [This paper presents a new model (Z-Line) for the representation of frequency-dependent multicircuit transmission lines in time-domain transient solutions].

Castellanos F., Marti J.R., Marcano F. (1997). Phase-domain multiphase transmission line models, *Electrical Power and Energy Systems* 19, 241-248. [This paper presents two line models, that circumvent the typical issue with frequency dependent transformation matrices representation in transient programs, by writing the propagation functions directly in the phase domain and thus avoiding the use of modal transformation matrices; the first model avoids the use of modal transformation matrices by separating the ideal-line traveling effect from the loss effects, and the second proposed model is a full frequency dependent distributed parameter model based on idempotent decomposition].

Chimklai S., Marti J.R. (1995). Simplified three-phase transformer model for electromagnetic transient studies, *IEEE Trans. on Power Delivery* 10, 1316-1325. [This presents a simplified high-frequency model for three-phase, two- and three-winding transformers, with the addition of the winding capacitances and the synthesis of the frequency-dependent short-circuit branch by an RLC equivalent network].

Chowdhuri P. (2003). *Electromagnetic Transients in Power Systems*, 2nd Edition, RS Press, John Wiley. [This book presents the basic theories of the generation and propagation of electromagnetic transients in power systems, discusses the performance of power apparatus under transient voltages and introduce the principles of protection against overvoltages].

CIGRE WG 33.02 (1990). Guidelines for Representation of Network Elements when Calculating Transients, CIGRE Brochure no. 39. [This brochure presents a review of guidelines proposed for representing power system components when calculating electromagnetic transients by means a computer].

Corzine K.A., Kuhn B.T., Sudhoff S.D., Hegner H.J. (1998). An improved method for incorporating magnetic saturation in the q-d synchronous machine model, *IEEE Trans. on Energy Conversion* 13, 270-275. [This paper describes a method of representing magnetic saturation using arctangent function. This method has several good features and requires only four parameters to completely specify the entire saturation characteristic. The saturation is implemented in the d-axis only].

Degeneff R.C. (2007). Transient-Voltage Response, Chapter 20 in *Power Systems* (L.L. Grigsby, Ed.), Boca Raton, FL: CRC Press. [This chapter presents an introduction to transformer winding models for very fast transient analysis, describes the procedures for determining the parameters to be specified in those models, and summarizes different methods that can be applied for solution of transient response, including internal winding resonances].

Degeneff R.C. (1977). A general method for determining resonances in transformer windings, *IEEE Trans. on Power Apparatus Systems* 96, 423-430. [This paper presents a method for calculating terminal and internal impedance versus frequency for a lumped parameter model of a transformer].

De Leon F., Semlyen A. (1995). A simple representation of dynamic hysteresis losses in power transformers, *IEEE Trans. on Power Delivery* 10, 315–321: [This paper describes a procedure for the representation of hysteresis in the laminations of power transformers in the simulation of electromagnetic transient phenomena].

De León F., Semlyen A. (1993). Time domain modeling of eddy current effects for transformer transients, *IEEE Trans. on Power Delivery* 8, 271 280. [Comprehensive discussion of existing analytical formulae for the calculation of losses in the windings of a power transformer for the study of electromagnetic transients].

De León F., Gómez P., Martinez-Velasco J.A., Rioual M. (2009). Transformers, Chapter 4 of *Power System Transients. Parameter Determination*, J.A. Martinez-Velasco (ed.), Boca Raton, FL: CRC Press. [This chapter details the type of transformer models to be used in transient analysis and simulation, and presents procedures for determining the parameters to be specified in those models].

Deri A., Tevan G., Semlyen A., Castanheira A. (1981). The complex ground return plane. A simplified model for homogeneous and multi-layer earth return, *IEEE Trans. on Power Apparatus and Systems* 100, 3686-3693. [This paper introduces, for modeling current return in homogeneous ground, the concept of an ideal (superconducting) current return plane placed below the ground surface at a complex distance equal to the complex penetration depth for plane waves].

Dick E.P., Cheung R.W., Porter J.W. (1991). Generator models for overvoltages simulations, *IEEE Trans. on Power Delivery* 6, 728-735. [This paper presents generator winding models for simulating dielectric stresses arising from 5 - 50 kHz oscillatory transients and from steep-fronted surges].

Dick E.P., Gupta B.K., Pillai P., Narang A., Sharma D.K. (1988). Equivalent circuits for simulating switching surges at motor terminals, *IEEE Trans. on Energy Conversion* 3, 696-704. [This paper presents equivalent circuits for use in simulating steep-fronted surge propagation from a circuit breaker to the terminals of a motor].

Dommel H.W. (1986). *EMTP Theory Book*, Portland, OR, USA: Bonneville Power Administration. [This book presents the fundamentals of the electro-magnetic transient program solution approach as well as describes many details of modeling and representing various components].

Dugan R.C., Brown G.W., Rocamora R.G. (1977). Surge propagation in three-phase pipe-type cables, Part II – Duplication of field tests including the effects of neutral wires and pipe saturation, *IEEE Trans. on Power Apparatus and Systems* 96, 826-833. [This paper presents an analytical model of field tests of surge propagation in 69-kV pipe-type cables, applying the solution techniques for any waveshape or travel time, and considering the effects of shield tape, skid wires, and proximity effects in the cable elements].

Fitzgerald A.E., Kingsley C., Umans S.D. (2002). *Electric Machinery*, 6th Edition, New York, NY: McGraw-Hill. [This book presents the fundamentals of various electrical machines. It also shows the details of the induction machines rotor construction, which results in variable equivalent impedance of the rotor equivalent circuit for the double-cage and deep-rotor bar type machines].

Fuchs E.E., Yildirim D., Grady W.M. (2000). Measurement of eddy-current loss coefficient PEC-R, derating of single-phase transformers, and comparison with K-factor approach, *IEEE Trans. on Power Deliver* 15*y*, 148-154. [This paper presents new measurement techniques to determine the derating of single-phase transformers with full-wave diode and thyristor rectifier loads, when a power amplifier is used to supply sinusoidal currents of different frequencies for measuring eddy-current losses of a 25 kVA single-phase transformer under short-circuit conditions].

Galloway R.H., Shorrocks W.B., Wedepohl L.M. (1964). Calculation of electrical parameters for short and long polyphase transmission lines, *Proc. IEE* 111, 2051-2059. [This paper presents how the basic matrixes of the conductor system are derived for traveling-wave phenomena in polyphase systems, taking into account the effect of conductor geometry, conductor internal impedance and the earth-return path].

Gary C. (1976). Approche complète de la propagation multifilaire en haute frèquence par utilization des matrices complexes, *EDF Bulletin de la Direction des Ètudes et Recherches-Serie B* 3/4, 5-20. [This paper introduces the concept of complex ground return plane concept which is situated at a complex distance below the earth surface and can be used to replace the real earth to derive very simple formulae for self and mutual impedances under ground return conditions].

Gole A., Martinez-Velasco J.A., Keri A. (eds.) (1998). Modeling and Analysis of Power System Transients Using Digital Programs, IEEE Special Publication TP-133-0, IEEE Catalog No. 99TP133-0. [This special publication presents an introduction to time-domain solution of electromagnetic transients in power systems using a digital computer. The publication covers two main topics: solution techniques and modeling of power components].

Gole A.M., Menzies R.W., Turanli H.M., Woodford D.A. (1984). Improved interfacing of electrical machine models to electromagnetic transients programs, *IEEE Trans. on Power Apparatus and Systems* 103, 2446-2451. [This paper describes the interfacing of machine models with the EMTP external network using the Norton equivalent and a time-step relaxation for the voltages. A special compensating impedance is used to improve the interface].

Greenwood A. (1991). *Electrical Transients in Power Systems*, New York. NY: John Wiley. [A reference book for the analysis of transient processes in electrical power systems].

Guardado J.L., Carrillo V., Cornick K.J. (1995). Calculation of interturn voltages in machine windings during switching transients measured on terminals, *IEEE Trans. on Energy Conversion* 10, 87-94. [This paper presents a technique, based on the measurement of switching transients at the machine terminals, for calculating interturn voltages in machine windings during transient conditions].

Guardado J.L., Cornick K.J. (1989). A computer model for calculating steep-fronted surge distribution in machine windings, *IEEE Trans. Energy Conversion* 4, 95-101. [This paper presents a computer model for predicting the distribution of steep-fronted surges in the line-end coils of machine windings].

Guardado J.L., Flores J.A., Venegas V., Naredo J.L., Uribe F.A. (2005). A machine winding model for switching transients studies using network synthesis, *IEEE Trans. on Energy Conversion* 20, 322-328. [This paper describes a computer model for calculating the surge propagation in the winding of electrical machines. The model considers the winding as a combination of a multi-conductor transmission line and a network of lumped parameters. The frequency dependence of the winding electrical parameters is calculated and incorporated into the analysis by means of Foster and Cauer circuits].

Gustavsen B., Semlyen A. (1998a). Simulation of transmission line transients using vector fitting and modal decomposition, *IEEE Trans. on Power Delivery* 13, 605-614. [This paper introduces a fast and robust method for rational fitting of frequency domain responses, well suited for both scalar and vector transfer functions, resulting in increased computational efficiency for transmission line models using modal decomposition with frequency dependent transformation matrices].

Gustavsen B., Semlyen A. (1998b). Application of vector fitting to the state equation representation of transformers for simulation of electromagnetic transients, *IEEE Trans. on Power Delivery* 13, 834-842. [This paper presents an efficient methodology for transient modeling of power transformers based on measured or calculated frequency responses].

Gustavsen B., Semlyen A. (1998c). Calculation of transmission line transients using polar decomposition, *IEEE Trans. on Power Delivery* 13, 855-862. [The paper presents a new power transmission line model suitable for the calculation of electromagnetic transients on overhead lines and underground cables].

Gustavsen B., Sletbak J., Henriksen T. (1995). Calculation of electromagnetic transients in transmission cables and lines taking frequency dependent effects accurately into account, *IEEE Trans. on Power Delivery* 10, 1076-1084. [This paper presents a traveling wave model for power transmission cables and lines in which the frequency dependence of the modal transformation matrix is accurately taken into account].

Gustavsen B. (2002). Computer code for rational approximation of frequency dependent admittance matrices, *IEEE Trans. on Power Delivery* 17, 1093-1098. [This paper deals with the problem of approximating with rational functions a matrix whose frequency dependent elements have been obtained from calculations or from measurements].

Gustavsen B. (2004). Wide band modeling of power transformers, *IEEE Trans. on Power Delivery* 19, 414-422. [This paper describes the measurement setup and modeling technique used for obtaining a linear wide band frequency-dependent black box model of a two-winding power transformer, for the purpose of calculation of electromagnetic transients in power systems].

Gustavsen B., Noda T., Naredo J.L., Uribe F.A., Martinez-Velasco J.A. (2009). Insulated Cables, Chapter 3 of *Power System Transients. Parameter Determination*, J.A. Martinez-Velasco (ed.), Boca Raton, FL: CRC Press. [This chapter presents the procedures that must be applied for the estimation of parameters to be specified in insulated cable models for transient studies using a time-domain simulation tool. The chapter includes a discussion about the conversion procedures that must be required for application of routines implemented in present transients tools].

Gustavsen B. (2010). A hybrid measurement approach for wideband characterization and modeling of power transformers, *IEEE Trans. on Power Delivery* 25, 1932-1939. [This presents a hybrid procedure for wideband characterization and modeling of power transformer behavior from frequency sweep measurements].

Hatziargyriou N.D., Prousalidis J.M., Papadias B.C. (1993). Generalised transformer model based on the analysis of its magnetic core circuit, *IEE Proc.-C* 140, 269-278. [This paper presents a new transformer model, named `geometrical', based on the circuit analysis of its magnetic core, whose methodology is general and can be used for any type of multiphase multiwinding transformer].

Hileman A.R. (1999). *Insulation Coordination for Power Systems*, New York, NY: Marcel Dekker. [A detailed and comprehensive reference book for power system insulation coordination].

Hung R., Dommel H.W. (1996). Synchronous machine models for simulation of induction motor transients, *IEEE Trans. on Power Systems* 11, 833-838. [This paper presents the details of using the existing EMTP synchronous machine model to simulate induction motor transients. The saturation of the main magnetizing flux and possible implementation of the saturation of the leakage inductances is also discussed].

Husianycia Y., Rioual M. (2006). Determination of the residual fluxes when de-energizing a power transformer. Comparison with on site tests, *IEEE PES General Meeting*, San Francisco. [This paper describes the determination of the residual fluxes, when opening the circuit-breaker poles, the phenomena involved, and the comparison with on site tests made on a 200 MVA step-up transformer of a hydraulic power plant].

IEC 60071-1 (2010). Insulation co-ordination, Part 1: Definitions, principles and rules. [This standard specifies the procedure for the selection of the rated withstand voltages for the phase-to-earth, phase-to-phase and longitudinal insulation of the equipment and the installations of three-phase a.c. systems having a highest voltage for equipment above 1 kV].

IEC 60071-2 (1996). Insulation co-ordination, Part 2: Application guide. [This standard presents an application guide for the selection of insulation levels of equipment or installations for three-phase electrical systems with nominal voltages above 1 kV].

IEC TR 60071-4 (2004). Insulation co-ordination - Part 4: Computational guide to insulation co-ordination and modelling of electrical networks. [This standard provides guidance on conducting insulation co-ordination studies which propose internationally recognized recommendations - for the numerical modeling of electrical systems, and - for the implementation of deterministic and probabilistic methods adapted to the use of numerical programs].

IEEE Slow Transients Task Force of IEEE Working Group on Modeling and Analysis of System Transients using Digital Programs (1995). Modeling and analysis guidelines for slow transients. Part I. Torsional oscillations; transient torques; turbine blade vibrations; fast bus transfer, *IEEE Trans. on Power Delivery* 10, 1950-1955. [This paper describes a method for implementing mechanical system as a multi-mass lumped-parameter spring–mass system. The order of the system and its coefficients can be selected to appropriately represent the mechanical dynamics of the machine's shafts, which is needed to accurately representing the slow transients and sub-synchronous resonances].

IEEE Std 1313.2 (1999). IEEE Guide for the Application of Insulation Coordination. [This standard presents a guide for the calculation method for selection of phase-to-ground and phase-to-phase insulation withstand voltages for equipment, giving methods for insulation coordination of different air-insulated systems like transmission lines and substations].

Ikeda M., Hiyama T. (2007). Simulation studies of the transients of squirrel-cage induction motors, *IEEE Trans. on Energy Conversion* 22, 233-239. [This paper proposes a new simulation approach in consideration of a saturation and a deep bar effect for the study of transients of three-phase squirrel-cage type induction motors].

Jatskevich J., Pekarek S.D., Davoudi A. (2006). Parametric average-value model of synchronous machine-rectifier systems, *IEEE Trans. on Energy Conversion* 21, 9-18. [This paper proposes a new average-value model of a rectifier circuit in a synchronous-machine-fed system. The proposed approach utilizes a proper state model of the synchronous machine in the qd-rotor reference frame, whereas the rectifier/dc-link dynamics are represented using a suitable proper transfer function and a set of non-linear parametric functions that are readily established numerically].

Karaagac U., Mahseredjian J., Saad O., Dennetière S. (2011). Synchronous machine modeling precision and efficiency in electromagnetic transients, *IEEE Trans. on Power Delivery* 26, 1072-1082. [This paper describes several methods for improving the interface of conventional qd0 machine models with the external EMTP network. The interface is shown to be improved by allowing internal to the machine model (fractional) iterations or time steps that are between the two existing main network solution points. The authors also propose to use the hybrid qd0-PD and qd0-VBR models that can switch between the PD and qd0 models and qd0 and VBR models, respectively].

Karaagac U., Mahseredjian J., Saad O. (2011). An efficient synchronous machine model for electromagnetic transients, *IEEE Trans. on Power Delivery* 26, 2456-2465. [This paper describes a hybrid qd0-PD model that uses prediction-correction iterations and achieves a constant admittance sub-matrix, which can eliminate the need for switching between the models and improves the interfacing accuracy].

Krause P.C., Thomas C.H. (1965). Simulation of symmetrical induction machinery, *IEEE Trans. on Power Apparatus and Systems* 84, 1038-1053. [This paper generalizing several commonly used reference frames into a unified arbitrary reference frame theory that has been very actively used for the analysis of electrical machinery, motor drives and controls. It is shown that any reference frame can be obtained by assigning a particular speed to the arbitrary reference frame].

Krause P.C., Wasynczuk O., Sudhoff S.D. (2002). *Analysis of Electric Machinery and Drive Systems*, 2nd Edition, Piscataway, NJ: IEEE Press. [This book presents the fundamentals and classical analysis of electric machinery and drive systems. The presented general-purpose full-order machine models are based on the coupled-circuit representation of the machine's windings, which is generally considered sufficient for the systems transients and motor-drive control applications].

Kundur P. (1994). *Power System Stability and Control*, New York, NY: McGraw-Hill. [This book contains the fundamentals of the electrical machine models (full and reduced order) that are generally accepted for the power systems transient and transient stability studies].

Lauw H.K., Meyer W.S. (1982). Universal machine modeling for the representation of rotating electrical machinery in an electromagnetic transients program, *IEEE Trans. on Power Apparatus and Systems* 101, 1342-1351. [This paper presents a compensation-based method of interfacing non-linear devices and machines models with the external network and the EMTP solution].

Levi E. (1995). A unified approach to main flux saturation modeling in D-Q axis models of induction machines, *IEEE Trans. on Energy Conversion* 10, 455-461. [This paper attempts to unify main flux saturation modeling in d-q axis models of induction machines by presenting a general method of saturation modeling. Selection of state-space variables in the saturated machine model is arbitrary and appropriate models in terms of different state-space variables result by application of the method].

Levi E. (1998). State-space d-q axis models of saturated salient pole synchronous machines, *IEE Proc.-Electr. Power Appl*. 145, 206-216. [A single saturation factor approach is presented and utilized for main flux saturation representation. Two distinct types of saturated machine models are identified, and a procedure is described that enables the formation of a number of similar but equivalent state-space models. A number of models are given in the final developed form].

Levi E. (1999). Saturation modeling in D-Q axis models of salient pole synchronous machines, *IEEE Trans. on Energy Conversion* 14, 44-50. [This paper presents several models where the state variables are selected in different ways. The paper describes the concept of generalized flux and generalized inductance, and applies it to the salient pole synchronous machines. The main flux saturation is represented for by the means of a single saturation factor approach and conversion of anisotropic machine to an equivalent isotropic machine is presented as well].

Lupo G., Petrarca C., Vitelli M., Tucci V. (2002). Multiconductor transmission line analysis of steep-front surges in machine windings, *IEEE Trans. on Dielectrics and Electrical Insulation* 9, 467-478. [This paper presents the modeling and simulation of a system, composed of a feeder cable and a stator winding, by using multi-conductor transmission line theory, in order to fulfill the numerical evaluation of the electrical stress in the line-end coil of the stator winding of a medium voltage motor fed by a pulsed width modulated (PWM) inverter which seems to be indispensable for a rational design of the machine].

Mahseredjian J., Dennetière S., Dubé L., Khodabakhchian B., Gérin-Lajoie L. (2007). On a new approach for the simulation of transients in power systems, *Electric Power Systems Research* 77, 1514-1520. [This paper presents a new simulation tool with a new graphical user interface and a new computational engine, with a new matrix formulation for computing load-flow, steady state and time-domain solutions].

Marti J.R. (1982). Accurate modeling of frequency-dependent transmission lines in electromagnetic transient simulations, *IEEE Trans. on Power Apparatus Systems* 101, 147-155. [This paper presents a numerical approximation technique for solving the time-domain equations over the entire frequency range of a frequency-dependent distributed-parameter transmission line].

Marti L. (1988). Simulation of transients in underground cables with frequency-dependent modal transformation matrices, *IEEE Trans. on Power Delivery* 3, 1099-1110. [This paper presents a new model of underground high-voltage cables for the simulation of electromagnetic transients].

Martinez J.A., Mork B. (2005). Transformer modeling for low- and mid-frequency transients - A review, *IEEE Trans. on Power Delivery* 20, 1625-1632. [This paper presents a review of transformer models for simulation of low- and mid-frequency transients, and a discussion about the estimation of parameters].

Martinez J.A., Walling R., Mork B., Martin-Arnedo J., Durbak D. (2005). Parameter determination for modeling systems transients. Part III: Transformers 20, *IEEE Trans. on Power Delivery*, 2051-2062. [This paper provides guidelines for the estimation of transformer model parameters for low- and mid-frequency transient simulations].

Martinez-Velasco J.A. Basic Methods for Analysis of High Frequency Transients in Power Apparatus Windings, in *Electromagnetic Transients in Transformer and Rotating Machine Windings*, C. Su (ed.), IGI Global, to be published. [This chapter introduces basic models for analyzing the response of power apparatus windings to steep-fronted voltage surges].

Martinez-Velasco J.A. (2009), Parameter Determination for Electromagnetic Transient Analysis in Power Systems, Chapter 1 of *Power System Transients. Parameter Determination*, J.A. Martinez-Velasco (ed.), Boca Raton, FL: CRC Press. [This chapter presents a summary on the current status of procedures to be performed for deriving the mathematical representation of the most important power components in electromagnetic transient simulations].

Martinez-Velasco J.A., Ramirez A.I., Dávila M. (2009). Overhead Lines, Chapter 2 of *Power System Transients. Parameter Determination*, J.A. Martinez-Velasco (ed.), Boca Raton, FL: CRC Press. [This chapter details the different models that can be used for representing the various part of overhead transmission lines (conductors, shield wires, towers, insulators, footing impedances) in transient analysis and simulation, and presents procedures for determining the parameters to be specified in those models].

McLaren P.G., Oraee H. (1985). Multiconductor transmission line model for the line end coil of large AC machines, *Proc. IEE* 132, 149-156. [This paper describes the application of finite-elements field package to calculate the distributed L and C parameters of a multiconductor transmission-line model for the line-end coil of a large AC motor].

McNutt W.J., Blalock T.J., Hinton R.A. (1974). Response of transformer windings to system transient voltages, *IEEE Trans. on Power Apparatus and Systems* 93, 457-466. [This paper takes a tutorial approach to relate a transformer winding to an equivalent electrical network which can exhibit resonant effects both at its terminals and internally].

Meyer W.S., Dommel H.W. (1974). Numerical modeling of frequency dependent transmission-line parameters in an electromagnetic transients program, *IEEE Trans. on Power Apparatus Systems* 93, 1401-1409. [This paper emphasizes modeling aspects crucial to accurate and efficient numerical solution by digital computer, as part of a production electromagnetic transients program].

Morched A., Gustavsen B., Tartibi M. (1999). A universal model for accurate calculation of electromagnetic transients on overhead lines and underground cables 14, *IEEE Trans. on Power Delivery*, 1032-1038. [This paper presents a transmission line model, which can be applied to both overhead lines and cables even in the presence of a strongly frequency dependent transformation matrix and widely different modal time delays, for the simulation of electromagnetic transients in power systems].

Morched A., Marti L., Ottevangers J. (1993). A high frequency transformer model for the EMTP, *IEEE Trans. on Power Delivery* 8, 1615-1626. [This paper presents a black-box model to simulate the high-frequency behavior of a power transformer].

Mork B.A. (1999). Five-legged wound-core transformer model: Derivation, parameters, implementation, and evaluation, *IEEE Trans. on Power Delivery* 14, 1519-1526. [This presents an equivalent circuit for the widely used three-phase grounded-wye to grounded-wye five-legged wound-core distribution transformer].

Mork B.A., Gonzalez F., Ishchenko D., Stuehm D.L., Mitra J. (2007). Hybrid transformer model for transient simulation - Part I: Development and parameters, *IEEE Trans. on Power Delivery* 22, 248-255. [This paper presents a new topologically-correct hybrid transformer model developed for low- and mid-frequency transient simulations].

Nakanishi H., Ametani A. (1986). Transient calculation of a transmission line using superposition law, *IEE Proc* 133, 263-269. [This paper presents a method of calculation of transmission line transients using the superposition law].

Narang A., Brierley R.H. (1994). Topology based magnetic model for steady-state and transient studies for three-phase core type transformers, *IEEE Trans. on Power Systems* 9, 1337-1349. [This paper presents a formulation to build a topological model for three-phase core type transformers based on normally available test data].

Naredo J.L., Soudack A.C., Martí J.R. (1995). Simulation of transients on transmission lines with corona via the method of characteristics, *IEE Proc. Gener. Transm. Distrib.* 142, 81-87. [This paper reports the first successful application of the eigenvector method of characteristics to nonlinear transients on lines].

Nguyen H.V., Dommel H.W., Marti J.R. (1997). Direct phase-domain modeling of frequency-dependent overhead transmission lines, *IEEE Trans. on Power Delivery* 12, 1335-1342. [This paper presents a new wideband transmission line model, based on synthesizing the line functions directly in the phase domain, including the complete frequency-dependent nature of untransposed overhead transmission lines, and designed to be implemented in general electromagnetic transients programs such as the EMTP].

Noda T. (2008). Numerical techniques for accurate evaluation of overhead line and underground cable constants, *Trans. on Electrical and Electronic Engineering* 3, 549-559. [This paper presents some techniques as elements for accurately calculating the transmission line constants].

Noda T., Nagaoka N., Ametani A. (1996). Phase domain modeling of frequency-dependent transmission lines by means of an ARMA model, *IEEE Trans. on Power Delivery* 11, 401-411. [This paper presents a method for time-domain transient calculation in which frequency-dependent transmission lines and cables are modeled in the phase domain rather than in the modal domain].

Noda T., Nagaoka N., Ametani A. (1997). Further improvements to a phase-domain ARMA line model in terms of convolution, steady-state initialization, and stability, *IEEE Trans. on Power Delivery* 12, 1327-1334. [This paper presents further improvements to a phase-domain ARMA (auto-regressive moving average) line model that is implemented in the ATP version of EMTP].

Noualy J.P., Le Roy G. (1977). Wave-propagation modes on high-voltage cables, *IEEE Trans. on Power Apparatus and Systems* 96, 158-165. [This paper presents a methodology for analyzing wave-propagation modes in three underground single-core cables and a simplified method for working out propagation parameters].

Pekarek S.D., Wasynczuk O., Hegner H.J. (1998). An efficient and accurate model for the simulation and analysis of synchronous machine/converter systems, *IEEE Trans. on Energy Conversion* 13, 42-48. [This paper for the first time presents the full-order voltage-behind-reactance synchronous machine model for the state-variable-based simulation languages. The original model has rotor-position-dependent inductance as well as resistance matrices. The model is demonstrated on machine-rectifier system implemented in the ASMG].

Pollaczek F. (1926). On the field produced by an infinitely long wire carrying alternating current, (in German), *Elektrische Nachrichtentechnik* 3, 339-359. [This paper presents the calculation of the electromagnetic field produced by an infinitely long wire that carries alternating current and is parallel to ground for which a finite conductivity is assumed].

Pollaczek F. (1927). On the induction effects of a single phase ac line, (in German), *Elektrische Nachrichtentechnik* 4, 18-30. [This paper is a continuation of the previous paper by the same author].

Popov M., van der Sluis L., Paap G.C., de Herdt H. (2003). Computation of very fast transient overvoltages in transformer windings, *IEEE Trans. on Power Delivery* 18, 1268-1274. [This paper uses a hybrid model which is a combination of the multi-conductor transmission line model (MTLM) and the single-transmission line model (STLM) for the computation of very fast transient overvoltages (VFTOs) in transformer windings].

Popov M., van der Sluis L., Smeets R.P.P., Lopez Roldan J. (2007). Analysis of very fast transients in layer-type transformer windings, *IEEE Trans. on Power Delivery* 22, 238-247. [This paper deals with the measurement, modeling, and simulation of very fast transient overvoltages in layer-type distribution transformer windings].

Ragavan K., Satish L. (2005). An efficient method to compute transfer function of a transformer from its equivalent circuit, *IEEE Trans. on Power Delivery* 20, 780-788. [This paper presents a novel solution based on state space analysis approach, showing how the linearly transformed state space formulation, together with algebraic manipulations, can become useful].

Ramírez A. I., Naredo J. L., Moreno P. (2005). Full frequency dependent line model for electromagnetic transient simulation including lumped and distributed sources, *IEEE Trans. on Power Delivery*, 20, No. 1, pp 292-299. [In this paper an extension of the method of characteristics is presented for modeling multi-conductor lines an cables with full frequency-dependent features. This model is suitable for including distributed EM sources and corona effect].

Reckleff J.G., Nelson J.K., Musil R.J., Wenger S. (1988). Characterization of fast rise-time transients when energizing large 13.2 kV motors, *IEEE Trans. on Power Delivery* 3, 627-636. [This paper reports results of an investigation of transients associated with energizing large 13.2 kV motors, 3000 to 13500 hp].

Rhudy R.G., Owen E.L., Sharma D.K. (1986). Voltage distribution among the coils and turns of a form wound ac rotating machine exposed to impulse voltage, *IEEE Trans. on Energy Conversion* 1, 50-60. [This paper describes a method of calculating voltage distribution in a stator winding exposed to impulse voltage. The winding is treated as an infinite number of identical coils connected in series, with each coil represented by an equivalent circuit including inductance, turn-to-ground capacitance and conductance, and with mutual inductance, capacitance, and conductance between turns].

Rioual M., Bernin B., Crepy C. (2010). Determination of transient phenomena when energizing a 340 MVA transformer having a highly non linear characteristic: Modeling and their validation by on site tests, *IEEE PES General Meeting*, Minneapolis. [This paper describes the calculation of the air core reactance for a power transformer, determined from analytical formulas, and validated by on site tests performed involving its energization].

Rioual M., Sicre, C. (2000). Energization of a no-load transformer for power restoration purposes: Modeling and validation by on site tests, *IEEE PES Winter Meeting*, Singapore. [This paper describes a detailed modeling of the power system for restoration purposes, and its validation by on site tests].

Rivas R.A., Marti J.R. (2002). Calculation of frequency-dependent parameters of power cables: Matrix partitioning techniques, *IEEE Trans. on Power Delivery* 17, 1085-1092. [This paper presents a new algorithm for the calculation of the frequency-dependent parameters of arbitrarily shaped power cable arrangements].

Schelkunoff S.A. (1934). The electromagnetic theory of coaxial transmission lines and cylindrical shields, *Bell Syst. Tech. Journal* 13, 532-579. [This paper expanded the theory of wave propagation along coaxial lines and cylindrical shields to cover systems with a plurality of coaxial conductors, including the effect of shielding and crosstalk, and adapted the theory to engineering uses considering the theory of electric circuits].

Semlyen A., Dabuleanu A. (1975). Fast and accurate switching transient calculations on transmission lines with ground return using recursive convolutions, *IEEE Trans. on Power Apparatus Systems* 94, 561-571. [This paper presents a new approach to the calculation of transients on transmission lines with frequency-dependent parameters].

Shibuya Y., Fujita S., Tamaki E. (2001). Analysis of very fast transients in transformer, *IEE Proc. C, Gen. Trans. Dist.* 148, 377-383. [This paper presents a practical method to calculate the high-frequency transients in the transformer winding based on multiconductor transmission-line theory].

Slemon G.R. (1953). Equivalent circuits for transformers and machines including non-linear effects, *Proc. IEE* 100, 129-143. [This paper presents a simple method whereby appropriate equivalent circuits may be developed for transformers and rotating machines].

Smith A.C., Healey R.C., Williamson S. (1996). A transient induction motor model including saturation and deep-rotor-bar effect, *IEEE Trans. on Energy Conversion* 11, 8-15. [A comprehensive review of transient cage induction motor models for use in inverter-fed drives and controllers].

Soysal A.O., Semlyen A. (1993). Practical transfer function estimation and its application to wide frequency range representation of transformers, *IEEE Trans. on Power Delivery* 8, 1627-1637. [This paper presents a widely applicable, general methodology for estimation of transfer function parameters from frequency response data].

Sudhoff S.D., Aliprantis D.C., Kuhn B.T., Chapman P.L. (2003). Experimental characterization procedure for use with an advanced induction machine model, *IEEE Trans. on Energy Conversion* 18, 48-56. [This paper presents the advanced induction machine model where the rotor is represented as a high-order transfer function of desired order to match the frequency response of the rotor circuit. The paper also presents the experimental procedure for determining the model parameters form measurements].

Tarasiewicz E.J., Morched A.S., Narang A., Dick E.P. (1993). Frequency dependent eddy current models for nonlinear iron cores, *IEEE Trans. on Power Systems* 8, 588 597. [This paper presents frequency dependent representations of eddy currents in laminated cores of power transformers].

Walling R.A., Barker K.D., Compton T.M., Zimmerman I.E. (1993). Ferroresonant overvoltages in grounded padmount transformers with low-loss silicon-steel cores, *IEEE Trans. on Power Delivery* 8, 1647-1660. [This paper describes the results of an extensive test program which determines that overvoltages are directly related to the ratio of capacitive susceptance divided by core losses and that the conventional use of rated exciting current can be a misleading indicator of ferroresonance susceptibility].

Wang L., Jatskevich J. (2006). A voltage-behind-reactance synchronous machine model for the EMTP-type solution, *IEEE Trans. on Power Systems* 21, 1539-1549. [This paper for the first time proposes the voltage behind reactance model that is discretized for the EMTP solution. It is shown that the new discretized model requires significantly fewer calculations than the conventional phase-domain model, while both achieve direct interface with the external network and EMTP solution. It is also demonstrates that the new model has batter scaled discrete-time-domain eigenvalues, which contributes to the very good numerical accuracy achieved by this model].

Wang L., Jatskevich J., Pekarek S.D. (2008). Modeling of induction machines using a voltage-behind-reactance formulation, *IEEE Trans. on Energy Conversion* 23, 382-392. [This paper for the first time derives the exact full-order voltage behind reactance model for the symmetrical induction machines. The model is implemented and demonstrated in the state-variable simulation package].

Wang L., Jatskevich J., Dinavahi V., Dommel H.W., Martinez J.A., Strunz K., Rioual M., Chang G.W., Iravani R. (2010). Methods of interfacing rotating machine models in transient simulation programs, *IEEE Trans. on Power Delivery* 25, 891–903. [This paper discusses methods of interfacing the induction and synchronous machine models in commonly-used state-variable-based and EMTP-based transient simulators. The known methods of interfacing are classified into indirect and direct, and numerous examples from different simulation packages are described].

Wang L., Jatskevich J. (2010). Approximate voltage-behind-reactance induction machine model for efficient interface with EMTP network solution, *IEEE Trans. on Power Systems* 25, 1016-1031. [This paper fir the first time demonstrates that the discretized induction machine model can have a constant equivalent conductance matrix, which is very desirable for achieving the efficient EMTP solution. The, the authors present an approximate voltage-behind reactance induction machine model that also achieves a constant conductance matrix as well as significantly improved accuracy compared to the equivalent phase-domain model].

Wedepohl L.M., Nguyen H.V., Irwin G.D. (1996). Frequency-dependent transformation matrices for untransposed transmission lines using Newton-Raphson method, *IEEE Trans. on Power Systems* 11, 1538-1546. [A comprehensive discussion of the frequency-dependent aspects of transmission line transformation matrices along with their asymptotic behaviors at high and low frequencies].

Wedepohl L.M., Wilcox D.J. (1973). Transient analysis of underground power-transmission systems. System-model and wave-propagation characteristics, *Proc. IEE* 120, 253-260. [This paper presents a mathematical model suitable for the analysis of traveling-wave phenomena in underground power-transmission systems].

Weeks W.L., Min Diao Y. (1984). Wave propagation in underground power cable, *IEEE Trans. on Power Apparatus and Systems* 10, 2816-2826. [This paper presents calculations to evaluate the effects of the semiconducting screens, the conductors, and the surrounding earth on the propagation constants of electromagnetic waves in concentric underground power cables].

Woodford D.A., Gole A.M., Menzies R.W. (1983). Digital simulation of DC links and AC machines, *IEEE Trans. on Power Apparatus and Systems* 102, 1616-1623. [This paper describes earlier EMTDC program and the methods of interfacing the user specified models and disconnected sub-networks. The modeling of AC machines is described as being carried out outside of the network, where the authors can use state variables and variable time step. The machine appears as a Norton current source that is fed from the calculated phase voltages. The authors recognize that a small time step and a small resistor or capacitor may be required at the interface].

Wright M.T., Yang S.J., McLeay K. (1983). General theory of fast-fronted interturn voltage distribution in electrical machine windings, *Proc. IEE* 130, 245-256. [This paper presents a generalized method of analysis that is capable of predicting voltage distribution in coils due to fast-fronted surges].

Yin Y., Dommel H.W. (1989). Calculation of frequency-dependent impedances of underground power cables with finite element method, *IEEE Trans. on Magnetics* 25, 3025-3027. [This paper presents a finite-element method for the calculation of the frequency-dependent series impedances of underground power cables].

Zhou D., Marti J.R. (1994). Skin effect calculations in pipe-type cables using a linear current subconductor technique, *IEEE Trans. on Power Delivery* 9, 598-604. [This paper presents a new technique to accurately calculate frequency dependent underground cable parameters].

Biographical Sketches

Juan A. Martinez-Velasco was born in Barcelona (Spain). He received the Ingeniero Industrial and Doctor Ingeniero Industrial degrees from the Universitat Politècnica de Catalunya (UPC), Spain. He is currently with the Departament d'Enginyeria Elèctrica of the UPC. His teaching and research areas cover Power Systems Analysis, Transmission and Distribution, Power Quality and Electromagnetic Transients. He is an active member of several IEEE and CIGRE Working Groups. Presently, he is the chair of the IEEE WG on Modeling and Analysis of System Transients Using Digital Programs.

Juri Jatskevich received the M.S.E.E. and the Ph.D. degrees in Electrical Engineering from Purdue University, West Lafayette IN, USA, in 1997 and 1999, respectively. He was Post-Doctoral Research Associate and Research Scientist at Purdue University, as well as consulted for P C Krause and Associates, Inc. Since 2002, he has been a faculty member at the University of British Columbia, Vancouver, Canada, where he is now an Associate Professor of Electrical and Computer Engineering. Dr. Jatskevich is presently a Chair of IEEE CAS Power Systems & Power Electronic Circuits Technical Committee, Editor of IEEE Transactions on Energy Conversion, Editor of IEEE Power Engineering Letters, and Associate Editor of IEEE Transactions on Power Electronics. He is also chairing the IEEE Task Force on Dynamic Average Modeling, under Working Group on Modeling and Analysis of System Transients Using Digital Programs. His research interests include electrical machines, power electronic systems, modeling and simulation of electromagnetic transients.

Shaahin Filizadeh received the B.Sc. and M.Sc. degrees in electrical engineering from the Sharif University of Technology, Tehran, Iran, in 1996 and 1998, respectively, and the Ph.D. degree from the University of Manitoba, Winnipeg, MB, Canada, in 2004. He is currently an assistant professor with the Department of Electrical and Computer Engineering, University of Manitoba. His areas of interest include electromagnetic transient simulation, nonlinear optimization, and power-electronic applications in power systems and vehicle propulsion. Dr. Filizadeh is a registered professional engineer in the province of Manitoba.

Marjan Popov received his Ph.D. degree from Delft University of Technology, Delft, The Netherlands, in 2002. From 1993 to 1998, he worked for the University of Skopje in the group of power systems. In 1997, he took sabbatical leave as an academic visitor at the University of Liverpool, U.K., where he performed research in the field of SF6 arc modeling. Since 1998 he has been working at Delft University of Technology where at present he is associate professor in Electrical Power Systems. In 2010 Dr. Popov obtained the prestigious Dutch Hidde Nijland award for his research achievements in the field of Electrical Power Engineering in the Netherlands, and in 2011 obtained IEEE PES Prize Paper Award and IEEE Switchgear Technical Committee Prize Paper Award. His major fields of interest are in future power systems, large scale of power system transients, and intelligent protection for future power systems. Dr. Popov is a senior member of IEEE, a member of CIGRE and actively participates in a few CIGRE working groups.

Michel Rioual was born in Toulon (France) on May 25th, 1959. He received the Engineering Diploma from the "Ecole Supérieure d'Electricité" (Gif sur Yvette, France) in 1983. He joined the EDF company (R&D Division) in 1984, and worked on electromagnetic transients in networks until 1991. In 1992, he joined the Wound Equipment Group as Project Manager on rotating machines. In 1997, he joined the Transformer Group, as Project Manager on the transformers for nuclear plants, and now related to hydraulic power plants. He is a Senior Member of IEEE, belongs to CIGRE and to the SEE (Society of Electrical and Electronics Engineers in France).

José L. Naredo graduated in 1976 as Mechanical and Electrical Engineer from Universidad Anahuac, Mexico DF. In 1987 he obtained the M. A. Sc. degree and in 1992 the PhD degree, both at The University of British Columbia, B. C., Canada. From 1978 to 1994 he worked at IIE (Instituto de Investigaciones Electricas of Mexico) on research and development activities related to power system communications, power system transients and power system protections. In 1994 he became full professor at The Universidad de Guadalajara, Mexico. Since May 1997 to present, he is full professor at Cinvestav (Centro de Investigación y de Estudios Avanzados del IPN, Mexico). From February 2005 to April 2007 he was director of Cinvestav, Campus Queretaro, México. Since 1992 Dr. Naredo holds an appointment as

National Researcher granted by the Federal Government of Mexico. He is Senior Member of IEEE, where he chairs the Task Force on Frequency Domain Analysis of Power System Transients.